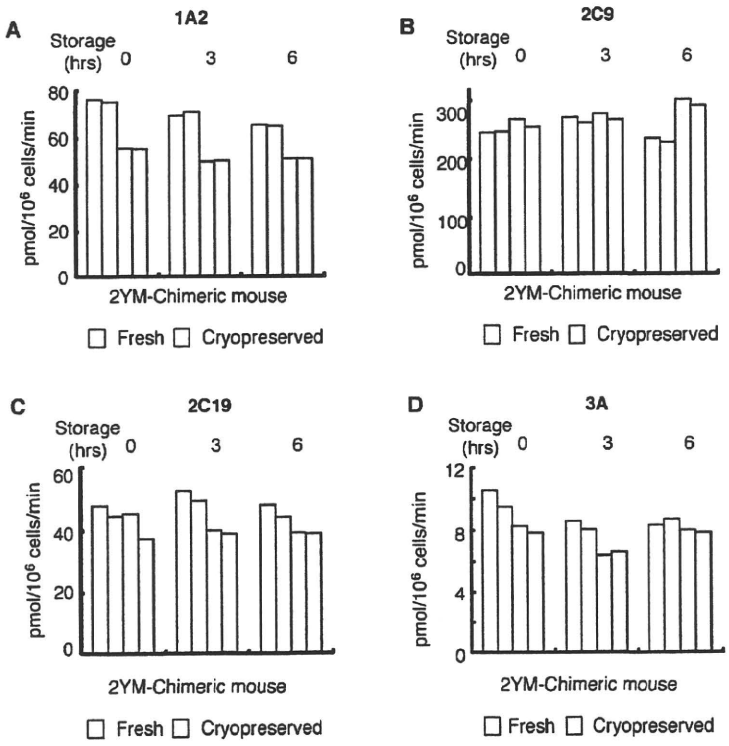

Fig. 2. Time course of P450 activities in fresh and cryopreserved chimeric hepatocytes after isolation or thawing, respectively, as assessed by HPLC

Fresh and cryopreserved 2YM-chimeric hepatocytes were stored after isolation and thawing, respectively, at 4°C for 3 and 6 h. The fresh and cryopreserved chimeric hepatocytes were purified by Percoll isodensity centrifugation after isolation or thawing. Fresh and cryopreserved chimeric hepatocytes, just after purification (0 h) and after storage for 3 h and 6 h, were treated with four substrates specific for four P450s (Table 1): (A) 1A2, (B) 2C9, (C) 2C19, and (D) 3A. The incubated medium was used to analyze each metabolite by HPLC; the metabolic activity of each P450 is shown as pmol/10^6 cells/min (Table 3).

cytes from the chimeric mice showed similar P450 activities to unpurified ones, supporting this suggestion (**Fig. 1**).

Glucuronide conjugation of ketoprofen in chimeric m-hepatocytes: Glucuronide conjugates were detected by *in vitro* metabolic assay for ketoprofen using fresh and cryopreserved hepatocytes from the 6YF-chimeric mouse and cryopreserved donor cells (6YF); however, uPA(wt/wt)/SCID mouse hepatocytes did not show products of UGT activity. The proportion of non-metabolized ketoprofen in fresh chimeric hepatocytes was similar to that in donor cells and lower than that in cryopreserved chimeric hepatocytes (**Fig. 4**). The proportion of ketoprofen-glucuronide in fresh chimeric hepatocytes was significantly higher than that of both cryopreserved chimeric hepatocytes ($P<0.05$). The transferred ketoprofen-glucuronide levels in fresh chimeric hepatocytes were also higher than those of both cells, but not significantly so (**Fig. 4**). From these results, we suggest that the freeze-thaw procedure decreased cellular glucuronide conjugation activities on drugs such as ketoprofen.

Discussion

Recent studies have revealed that chimeric mice may be a useful model for the examination of drug absorption, distribution, metabolism, and excretion (ADME) and drug interactions via enzyme induction and inhibition *in vivo*.[1,3,4,7,12–14] S-Warfarin has been shown to be metabolized to S-7-hydroxywarfarin, catalyzed by CYP2C9, and is primarily recovered in urine in humans.[15] The mass balance and metabolic disposition of S-warfarin in chimeric mice were found to be similar to reported human data.[14,16] In humans, ketoprofen is primarily metabolized by UGT and converted to ketoprofen glucuronides.[8] When chimeric mice were administered ketoprofen, glucuronide conjugates were detected in their sera and bile.[7] By treatment with typical inducers of P450 (3-methylcholanthrene and rifampicin), human CYP1A and CYP3A4, respectively, were induced in the chimeric mouse liver.[1,3] After treatment with quinidine, a specific inhibitor of human CYP2D6, the area under the curve (AUC) of CYP2D6 metabolites was significantly decreased in the chimeric mice, but not in

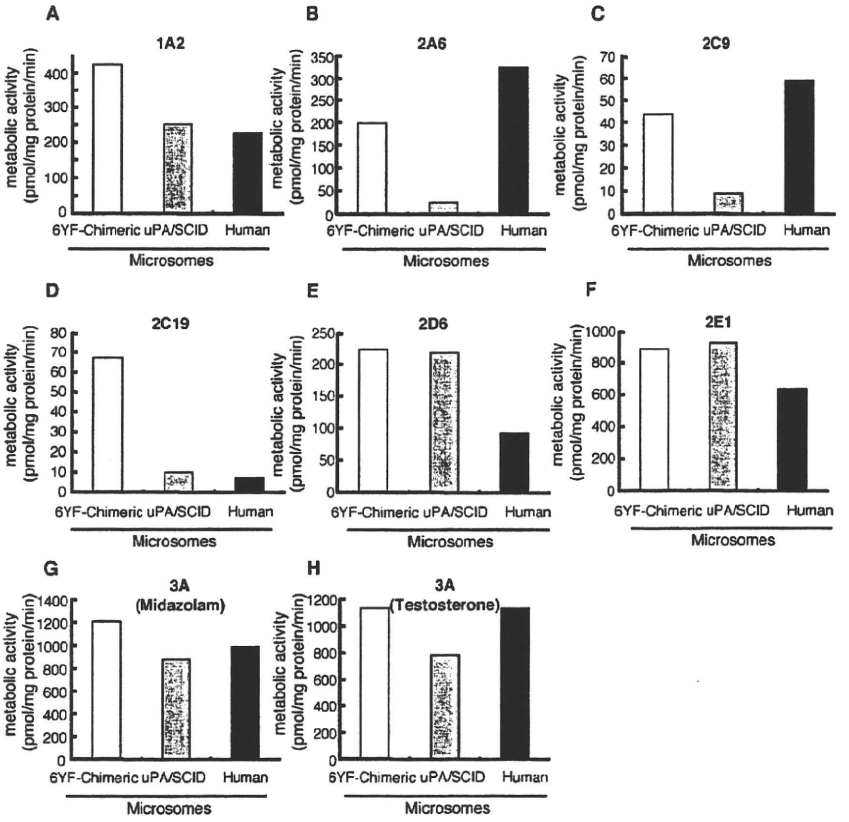

Fig. 3. P450 activities of liver microsomes from chimeric mice, uPA/SCID mice, and human livers as determined by LC-MS/MS
Microsomes from a 6YF-chimeric mouse and pooled microsomes of uPA/SCID mice and human livers were treated with eight substrates specific for seven P450s (Table 1), and the metabolite concentrations were measured by LC-MS/MS; the metabolic activity of each P450 is shown as pmol/mg protein/min (Table 2): (A) 1A2, (B) 2A6, (C) 2C9, (D) 2C19, (E) 2D6, (F) 2E1, (G) 3A, midazolam, and (H) 3A, testosterone.

control mice.[13] These findings demonstrate that h-hepatocytes in the chimeric mouse liver had normal human phase I and II enzyme activity, and that the chimeric mice may have advantages in studies of ADME and drug interactions. However, no study had examined the metabolic activity of fresh h-hepatocytes isolated from chimeric mice. In the present study, we determined whether the chimeric mouse could be a useful source of fresh h-hepatocytes for *in vitro* metabolic studies.

The metabolic capacities of fresh and corresponding cryopreserved hepatocytes from several donors have been compared by testosterone hydroxylation, 7-ethoxyresorufin-*O*-deethylase (EROD), and 7-ethoxycoumarin-*O*-deethylase (ECOD). These activities were found to be lower in cryopreserved hepatocytes than in fresh ones.[17,18] Phase II enzyme activities, GST, UGT toward 4-methylumbelliferone (MUF), and sulfotransferase (SULT) were also significantly reduced after cryopreservation of h-hepatocytes, whereas the activity of UGT toward 4-hydroxybiphenyl (HOBI) and that of SULT were similar to those measured in fresh h-hepatocytes.[17] Despite the observed reductions of these enzyme activities, cryopreserved h-hepatocytes are regarded as the best *in vitro* model for use in predicting human intrinsic clearance of xenobiotics.[19] This is because ahead-of-time experimental planning using fresh h-hepatocytes and attaining reproducible studies using the same donor of fresh h-hepatocytes is not feasible. Additionally, because large individual variations are known to exist among h-hepatocytes, pooled hepatocytes derived from several donors could help eliminate such individual variation, but such pooling of fresh h-hepatocytes is not possible. Here, we compared the P450 activities of fresh and cryopreserved chimeric hepatocytes originating from the same donor, and fresh h-hepatocytes from human livers. Results indicated that CYP1A2, 2C19, and 2D6 activities declined, while CYP2A6, 2C9, 2E1, and 3A activities were not affected by the freeze-thaw procedure. Fresh and cryopreserved chimeric h-hepatocytes were used for the determination of ketoprofen glucuronidation. Concentrations of ketoprofen-glucuronide and transferred ketoprofen-glucuronide were higher in fresh chimeric hepatocytes than in their cryopreserved counterparts. Chimeric hepatocytes from the same donor showed

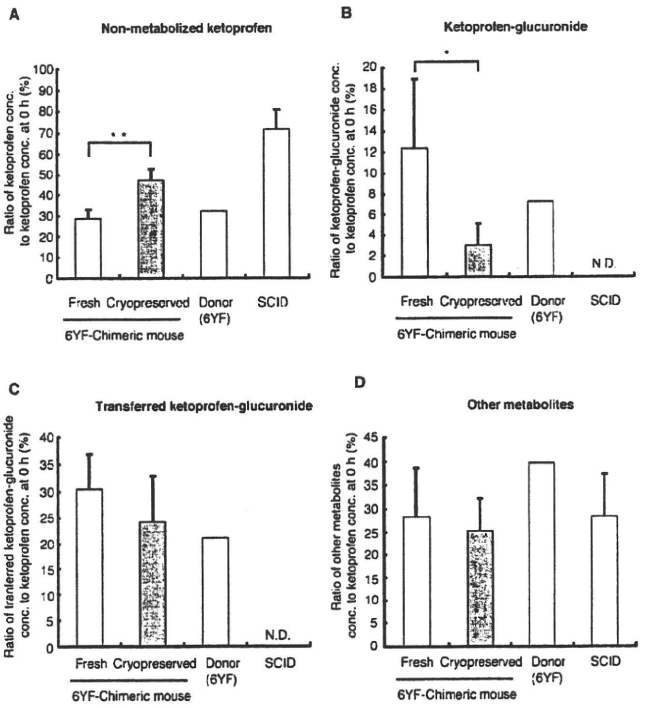

Fig. 4. Glucuronidation of ketoprofen in fresh and cryopreserved chimeric hepatocytes, uPA(wt/wt)/SCID mouse hepatocytes, and cryopreserved donor hepatocytes, as determined by LC-MS/MS
Fresh and cryopreserved chimeric hepatocytes, uPA(wt/wt)/SCID mouse hepatocytes, and cryopreserved donor hepatocytes (6YF) were incubated with ketoprofen for 3 h. The conditioned medium was treated with β-glucuronidase and 1 N KOH, and the concentration of ketoprofen was measured by LC-MS/MS (Table 2): (A) Non-metabolized ketoprofen, (B) Ketoprofen-glucuronide, (C) Transferred ketoprofen-glucuronide, and (D) other metabolites. The concentrations of ketoprofen-glucuronide and transferred ketoprofen-glucuronide were calculated by the formulas indicated in Materials and Methods, and the activities were expressed as the ratio of the concentration of ketoprofen or its glucuronide conjugate to the ketoprofen concentration at 0 h. The values shown are the means ± SD of three or five different chimeric mice. $^{*}p<0.05$, $^{**}p<0.01$. ND, not detected.

smaller variations in P450 activities than fresh h-hepatocytes from different individuals (**Fig. 1**). These results indicated that fresh chimeric hepatocytes may address the problem of individual differences in fresh h-hepatocytes. Additionally, the fresh and cryopreserved chimeric hepatocytes tested retained P450 (CYP1A2, 2C9, 2C19, and 3A) activities for at least 6 h. These studies demonstrated that chimeric mice can provide fresh h-hepatocytes ahead of time, making reproducible studies using the same donor possible.

The decreased metabolism in cryopreserved hepatocytes could be attributable to two mechanisms: inactivation of P450 enzymes and loss of the cofactor NADPH due to cell membrane damage.[20] The addition of a NADPH-generating system to the incubation mixture has been shown to increase benzo[a]pyrene metabolite formation by cryopreserved rat hepatocytes to approximately the level of freshly isolated rat hepatocytes.[21] When cryopreserved rat hepatocytes were purified by Percoll centrifugation after thawing, to remove dead and membrane-damaged cells, benzo[a]pyrene metabolism recovered to equal that of fresh rat hepatocytes.[21] The decline in phase II enzyme activities has also been shown to be overcome by Percoll centrifugation, but not completely to the level of freshly isolated cells.[21] Addition of endogenous cofactors uridine 5′-diphosphoglucuronic acid (UDPGA) and adenosine 3′-phosphate 5′-phosphosulfate (PAPS) to cryopreserved rat hepatocytes improved 7-hydroxycoumarin-glucuronide and 7-hydroxycoumarin-sulfate formation to levels observed in fresh hepatocytes.[22] The UDPGA and PAPS synthesis machineries may be damaged during freezing and thawing. Fresh or cryopreserved chimeric hepatocytes would be useful in clarifying the mechanisms underlying the decline in metabolic activities after freezing and thawing. The results of this study also suggest that fresh chimeric hepatocytes are useful for testing phase I and II reactions, including glucuronidation, without the need for Percoll purification or the addition of cofactors.

Chimeric hepatocytes contain about 17% of m-hepatocytes, and 66Z antibodies react specifically with m-hepatocytes. We purified h-hepatocytes from the chimer-

ic hepatocytes by 66Z rat IgG and magnetic bead-conjugated anti-rat IgG antibodies. After the magnetic removal of m-hepatocytes, the proportion of m-hepatocytes decreased to approximately 3%. We measured the P450 activities of microsomes isolated from the chimeric mouse and pooled microsomes from uPA/SCID mice and human livers using the same substrates as those used in the cell suspension study. Because we were not able to obtain microsomes from the donor of the chimeric mice (6YF), pooled human microsomes were used for this study. Except for CYP2D6 and 2E1, the activities of uPA/SCID mouse liver microsomes were similar to, or lower than, those of pooled human liver microsomes. The activities of CYP2D6 and 2E1 in uPA/SCID mouse liver microsomes were 50–100% higher than those of pooled human liver microsomes, respectively. We also found that P450 activities were similar between pre- and post-purified chimeric hepatocytes. From these results, we deduced that m-hepatocytes contaminating the chimeric hepatocytes might not significantly affect the activities of chimeric hepatocytes.

Gender differences in CYP3A4 activities have been reported when using cryopreserved human hepatocytes.[23] We assumed that P450 activities were independent of the gender in recipient uPA/SCID mice, because we recently showed that there was no significant difference in P450 activity (CYP1A2, 2C9. 2C19, 2D6, and 3A) between microsomes from male and female chimeric mice.[24] In the present study, hepatocytes isolated from both male and female chimeric mice were used, and there was no difference in P450 or UGT activity between them (data not shown); however, the number of animals was limited.

Non-platable 4YF- and 6YF-donor cells were engrafted and grown in the uPA/SCID mice and hepatocytes were isolated from the livers using the collagenase perfusion method. Fresh chimeric hepatocytes adhered well onto the culture dishes, compared with fresh and cryopreserved h-hepatocytes. This suggests that fresh chimeric hepatocytes would be suitable for P450 induction and toxicity studies that are usually performed with plated cells.

Cryopreserved h-hepatocytes isolated from the chimeric mice were demonstrated to be useful for evaluating the induction of CYP1A2 and 3A4;[25] in addition, CYP1A2 and 3A4 mRNA induction and expression from three different donor hepatocytes were reproduced in cryopreserved chimeric hepatocytes.[26] Due to the higher plating efficiency of fresh hepatocytes compared to cryopreserved cells, fresh chimeric hepatocytes would be useful for evaluating the human P450 induction abilities of xenobiotics.

We conclude that fresh and reproducible h-hepatocytes isolated from chimeric mice could be a useful tool in predicting the pharmacokinetics of chemical entities in addition to *in vivo* chimeric mouse studies. Comparative *in vitro* and *in vivo* studies using chimeric mice with the same donor could generate abundant data for resolving poorly understood phenomena and mechanisms.

Acknowledgments: We thank Mss. Y. Yoshizane, S. Nagai, and H. Kohno for providing excellent technical assistance.

References

1) Tateno, C., Yoshizane, Y., Saito, N., Kataoka, M., Utoh, R., Yamasaki, C., Tachibana, A., Soeno, Y., Asahina, K., Hino, H., Asahara, T., Yokoi, T., Furukawa, T. and Yoshizato, K.: Near completely humanized liver in mice shows human-type metabolic responses to drugs. *Am. J. Pathol.*, **165**: 901–912 (2004).
2) Katoh, M., Matsui, T., Nakajima, M., Tateno, C., Kataoka, M., Soeno, Y., Horie, T., Iwasaki, K., Yoshizato, K. and Yokoi, T.: Expression of human cytochrome P450 in chimeric mice with humanized liver. *Drug Metab. Dispos.*, **32**: 1402–1410 (2004).
3) Katoh, M., Matsui, T., Nakajima, M., Tateno, C., Soeno, Y., Horie, T., Iwasaki, K., Yoshizato, K. and Yokoi, T.: In vivo induction of human cytochrome P450 enzymes expressed in chimeric mice with humanized liver. *Drug Metab. Dispos.*, **33**: 754–763 (2005).
4) Katoh, M., Matsui, T., Okumura, H., Nakajima, M., Nishimura, M., Naito, S., Tateno, C., Yoshizato, K. and Yokoi, T.: Expression of human phase II enzymes in chimeric mice with humanized liver. *Drug Metab. Dispos.*, **33**: 1333–1340 (2005).
5) Wilkinson, G. R.: Drug metabolism and variability among patients in drug response. *N. Engl. J. Med.*, **352**: 2211–2221 (2005).
6) Populaire, P., Terlain, B., Pascal, S., Decouvelaere, B., Renard, A. and Thomas, J. P.: Biological behavior: serum levels, excretion and biotransformation of (3-benzoylphenyl)-2-propionic acid, or ketoprofen, in animals and men. *Ann. Pharm. Fr.*, **12**: 735–749 (1973).
7) Hashizume, K., Ohzone, Y., Adachi, Y., Ninomiya, A., Inoue, T. and Horie, T.: Characterization of chimeric mouse on in vivo metabolism of ketoprofen. *The Cell*, **40**: 26–29 (2008) in Japanese.
8) Ishizaki, T., Sasaki, T., Suganuma, T., Horai, Y., Chiba, K., Watanabe, M., Asuke, W. and Hoshi, H.: Pharmacokinetics of ketoprofen following single oral, intramuscular and rectal doses and after repeated oral administration. *Eur. J. Clin. Pharmacol.*, **18**: 407–414 (1980).
9) Ohashi, K., Tatsumi, K., Utoh, R., Takagi, S., Shima, M. and Okano, T.: Engineering liver tissues under the kidney capsule site provides therapeutic effects to hemophilia B mice. *Cell Transplant.*, in press
10) Sugihara, K., Kitamura, S., Yamada, T., Ohta, S., Yamashita, K., Yasuda, M. and Fujii-Kuriyama, Y.: Aryl hydrocarbon receptor (Ah)-mediated induction of xanthine oxidase/xanthine dehydrogenase activity by 2,3,7,8-tetrachlorodibenzo-p-dioxin. *Biochem. Biophys. Res. Commun.*, **281**: 1093–1099 (2001).
11) Nagano, M., Yamashita, S., Hirano, K., Ito, M., Maruyama, T., Ishihara, M., Sagehashi, Y., Oka, T., Kujiraoka, T., Hattori, H., Nakajima, N., Egashira, T., Kondo, M., Sakai, N. and Matsuzawa, Y.: Two novel missense mutations in the CETP gene in Japanese hyperalphalipoproteinemic subjects: high-throughput

assay by Invader assay. *J. Lipid Res.*, **43**: 1011–1018 (2002).
12) Kiyotani, K., Yamazaki, H., Fujieda, M., Iwano, S., Matsumura, K., Satarug, S., Ujjin, P., Shimada, T., Guengerich, F. P., Parkinson, A., Honda, G. Nakagawa, K., Ishizaki, T. and Kamataki, T.: Decreased coumarin 7-hydroxylase activities and CYP2A6 expression levels in humans caused by genetic polymorphism in CYP2A6 promoter region (CYP2A6*9). *Pharmacogenetics*, **13**: 689–695 (2003).
13) Katoh, M., Sawada, T., Soeno, Y., Nakajima, M., Tateno, C., Yoshizato, K. and Yokoi, T.: *In vivo* drug metabolism model for human cytochrome P450 enzyme using chimeric mice with humanized liver. *J. Pharm. Sci.*, **96**: 428–437 (2007).
14) Inoue, T., Nitta, K., Sugihara, K., Horie, T., Kitamura, S. and Ohta, S.: CYP2C9-catalyzed metabolism of S-warfarin to 7-hydroxywarfarin *in vivo* and *in vitro* in chimeric mice with humanized liver. *Drug Metab. Dispos.*, **36**: 2429–2433 (2008).
15) Rettie, A. E., Korzekwa, K. R., Kunze, K. L., Lawrence, R. F., Eddy, A. C., Aoyama, T., Gelboin, H. V., Gonzalez, F. J. and Trager, W. F.: Hydroxylation of warfarin by human cDNA-expressed cytochrome P-450: a role for P-4502C9 in the etiology of (S)-warfarin-drug interactions. *Chem. Res. Toxicol.*, **5**: 54–59 (1992).
16) Inoue, T., Sugihara, K., Ohshita, H., Horie, T., Kitamura, S. and Ohta, S.: Prediction of human disposition toward S-3H-warfarin using chimeric mice with humanized liver. *Drug Metab. Pharmacokinet.*, **24**: 153–160 (2009).
17) Steinberg, P., Fischer, T., Kiulies, S., Biefang, K., Platt, K. L., Oesch, F., Bottger, T., Bulitta, C., Kempf, P. and Hengstler, J.: Drug metabolizing capacity of cryopreserved human, rat, and mouse liver parenchymal cells in suspension. *Drug Metab. Dispos.*, **27**: 1415–1422 (1999).
18) Gebhardt, R., Hengstler, J. G., Muller, D., Glöckner, R., Buenning, P., Laube, B., Schmelzer, E., Ullrich, M., Utesch, D., Hewitt, N., Ringel, M., Hilz, B. R., Bader, A., Langsch, A., Koose, T., Burger, H. J., Maas, J. and Oesch, F.: New hepatocyte in vitro systems for drug metabolism: metabolic capacity and recommendations for application in basic research and drug development, standard operation procedures. *Drug Metab. Rev.*, **35**: 145–213 (2003).
19) Lau, Y. Y., Sapidou, E., Cui, X., White, R. E. and Cheng, K. C.: Development of a novel in vitro model to predict hepatic clearance using fresh, cryopreserved, and sandwich-cultured hepatocytes. *Drug Metab. Dispos.*, **30**: 1446–1454 (2002).
20) Hengstler, J. G., Utesch, D., Steinberg, P., Platt, K. L., Diener, B., Ringel, M., Swales, N., Fischer, T., Biefang, K., Gerl, M., Böttger, T. and Oesch, F.: Cryopreserved primary hepatocytes as a constantly available in vitro model for the evaluation of human and animal drug metabolism and enzyme induction. *Drug Metab. Rev.*, **32**: 81–118 (2000).
21) Diener, B., Utesch, D., Beer, N., Dürk, H. and Oesch, F.: A method for the cryopreservation of liver parenchymal cells for studies of xenobiotics. *Cryobiology*, **30**: 116–127 (1993).
22) Wang, Q., Jia, R., Ye, C., Garcia, M., Li, J. and Hidalgo, I. J.: Glucuronidation and sulfation of 7-hydroxycoumarin in liver matrices from human, dog, monkey, rat, and mouse. *In Vitro Cell Dev. Biol. Anim.*, **41**: 97–103 (2005).
23) Parkinson, A., Mudra, D. R., Johnson, C., Dwyer, A. and Carroll, K. M.: The effects of gender, age, ethnicity, and liver cirrhosis on cytochrome p450 enzyme activity in human liver microsomes and inducibility in cultured human hepatocytes. *Toxicol. Appl. Pharmacol.*, **199**: 193–209 (2004).
24) Kikuchi, R., McCown, M., Olson, P., Tateno, C., Morikawa, Y., Katoh, Y., Bourdet, D. L., Monshouwer, M. and Fretland, A. J.: Effect of hepatitis C virus infection on the mRNA expression of drug transporters and cytochrome p450 enzymes in chimeric mice with humanized liver. *Drug Metab. Dispos.*, **38**: 1954–1961 (2010).
25) Nishimura, M., Yokoi, T., Tateno, C., Kataoka, M., Takahashi, E., Horie, T., Yoshizato, K. and Naito, S.: Induction of human CYP1A2 and CYP3A4 in primary culture of hepatocytes from chimeric mice with humanized liver. *Drug Metab. Pharmacokinet.*, **20**: 121–126 (2005).
26) Yoshitsugu, H., Nishimura, M., Tateno, C., Kataoka, M., Takahashi, E., Soeno, Y., Yoshizato, K., Yokoi, T. and Naito, S.: Evaluation of human CYP1A2 and CYP3A4 mRNA expression in hepatocytes from chimeric mice with humanized liver. *Drug Metab. Pharmacokinet.*, **21**: 465–474 (2006).

Genes to Cells

DPPA4 modulates chromatin structure via association with DNA and core histone H3 in mouse embryonic stem cells

Hisaharu Masaki[1,2], Tomohiro Nishida[1a], Ryo Sakasai[1]* and Hirobumi Teraoka[1]

[1]*Department of Pathological Biochemistry, Medical Research Institute, Tokyo Medical and Dental University, Chiyoda-ku, Tokyo 101-0062, Japan*

[2]*Research Fellow of the Japan Society for the Promotion of Science, Japan*

Developmental pluripotency associated 4 (DPPA4) is one of the uncharacterized genes that is highly expressed in embryonic stem (ES) cells. DPPA4 is associated with active chromatin and involved in the pluripotency of mouse ES cells. However, the biological function of DPPA4 remains poorly understood. In this study, we performed fluorescence recovery after photobleaching (FRAP) analysis to examine the dynamics of DPPA4 in ES cells. FRAP analysis showed that the mobility of DPPA4 is similar to that of histone H1. In addition, biochemical analysis with purified proteins and immunoprecipitation analysis showed that DPPA4 directly binds to both DNA and core histone H3. The analysis using truncated proteins indicated that DPPA4 is associated with DNA via the N-terminal region and histone H3 via the C-terminal region. *In vitro* assembled chromatin showed resistance to micrococcal nuclease (MNase) digestion in the presence of DPPA4. Moreover, MNase assay and FRAP analysis with the truncated proteins implies that DPPA4 binding to both DNA and histone H3 is necessary for the chromatin structure resistant to MNase and for the proper localization of DPPA4 in ES cell nuclei. These results suggest that DPPA4 modulates the chromatin structure in association with DNA and histone H3 in ES cells.

Introduction

Mouse embryonic stem (ES) cells, derived from the inner cell mass of the blastocyst, have unlimited capacity for self-renewal and can differentiate into various cell types (Keller 2005). Moreover, human ES cells and induced pluripotent stem (iPS) cells have been established (Thomson *et al.* 1998; Takahashi *et al.* 2007; Yu *et al.* 2007). Thus, they are expected to become a valuable resource for stem cell therapy.

The pluripotency of mouse ES cells is maintained by the leukemia inhibitory factor (LIF) Jak/STAT3, bone morphogenic protein (BMP) Smad/Id, and Wnt/β-catenin signaling pathways (Burdon *et al.* 2002; Boiani & Schöler 2005). In addition, several transcription factors including Oct-3/4, Sox-2, Nanog, Sall4, and Klf family proteins play essential roles in mouse ES cell pluripotency (Chambers *et al.* 2003; Mitsui *et al.* 2003; Niwa *et al.* 2005; Zhang *et al.* 2006; Masui *et al.* 2007; Jiang *et al.* 2008). These signaling pathways and core transcription factors synergistically contribute to the maintenance of pluripotency in mouse ES cells, e.g., the LIF/Jak/STAT3 signaling pathway maintains ES cells in an undifferentiated state by the regulation of Klf4 gene expression (Niwa *et al.* 2009).

Genes involved in ES cell pluripotency and many other genes including Dppa4 (developmental pluripotency associated 4) are highly expressed during early mouse embryogenesis (Hamatani *et al.* 2004). Dppa4 is one of the genes originally identified as being highly expressed in early mouse embryo and ES cells (Bortvin *et al.* 2003). It has been reported that the expression of Dppa4 gene is potentially regulated by Oct-3/4 and Sox-2 in ES cells (Boyer *et al.* 2005; Chakravarthy *et al.* 2008). The expression of Dppa4 gene is restricted to early embryo and germ cells (Maldonado-Saldivia *et al.* 2007). DPPA4 has the SAP (SAF-A/B, Acinus and PIAS) domain, which is a putative

Communicated by: Kohei Miyazono
**Correspondence*: sakasai.pbc@mri.tmd.ac.jp
[a]*Present address*: Department of Stem Cell Medicine, Medical Research Institute, Tokyo Medical and Dental University, Chiyoda-ku, Tokyo 101-0062, Japan.

DOI: 10.1111/j.1365-2443.2010.01382.x
© 2010 The Authors
Journal compilation © 2010 by the Molecular Biology Society of Japan/Blackwell Publishing Ltd.

DNA-binding motif, and is considered to be involved in chromosomal organization, RNA processing, DNA repair, and apoptotic degradation of chromatin (Aravind & Koonin 2000). Several genes including Dppa4 have been identified by the RNAi screening against the requirement for self-renewal in mouse ES cells (Ivanova *et al.* 2006). Thus, it is considered that DPPA4 plays an important role in ES cells via association with chromatin. In fact, we have previously reported that DPPA4 associated with active chromatin is required for maintaining mouse ES cells in an undifferentiated state (Masaki *et al.* 2007).

Recent studies have revealed that unique chromatin states are maintained in ES cells. Major architectural chromatin proteins, such as histone H1, loosely bind to chromatin (Meshorer *et al.* 2006). The promoters of some developmental regulator genes have bivalent chromatin profiles in which both active (tri-methylation of histone H3 at lysine 4) and inactive (tri-methylation of histone H3 at lysine 27) chromatin marks are juxtaposed (Azuara *et al.* 2006; Bernstein *et al.* 2006). In addition, Polycomb repressive complex 2 (PRC2) binds to promoters of the developmental regulator genes and represses their transcription in ES cells (Boyer *et al.* 2006; Lee *et al.* 2006). The proteasome promotes a dynamic turnover of transcription factors and RNA polymerase II binding at tissue-specific genes, thereby restricting permissive transcriptional activity and keeping the genes in a potentiated state (Szutorisz *et al.* 2006). These reports indicate that ES cells have a unique open chromatin structure and suggest that pluripotency and differentiation are regulated by chromatin states. Thus, DPPA4 is associated with chromatin and possibly involved in the unique chromatin structure of ES cells.

In this study, to gain an insight into the molecular function of DPPA4 in mouse ES cells, we investigated the behavior of DPPA4 by fluorescence recovery after photobleaching (FRAP) analysis. Interestingly, FRAP analysis showed that the mobility of DPPA4 was similar to that of histone H1. Purified recombinant DPPA4 protein directly binds to DNA and core histones *in vitro*, and immunoprecipitation analysis showed the binding between DPPA4 and histone H3 in ES cells. The analysis of truncated DPPA4 proteins revealed that DPPA4 binds to DNA and histone H3 via the N-terminal and C-terminal regions, respectively. Furthermore, the addition of DPPA4 into *in vitro* reconstituted chromatin resulted in an increased resistance to micrococcal nuclease (MNase) digestion. Based on these results, we proposed a model that DPPA4 modulates the chromatin structure in association with DNA and histone H3 in ES cells.

Results

DPPA4 shows similar dynamics to linker histone H1

DPPA4 is involved in the maintenance of pluripotency in ES cells, but its function remains to be clarified. The putative SAP DNA-binding domain of DPPA4 raises a possibility that DPPA4 contributes to DNA metabolism through binding to chromatin. To investigate the molecular function of DPPA4 on chromosomal organization, we analyzed the dynamic property of DPPA4 and compared it with that of histones in living ES cells using FRAP analysis. As a preliminary experiment for FRAP analysis, the localization of DPPA4-EGFP (enhanced green fluorescent protein [GFP]) fusion protein was compared with that of endogenous DPPA4 by chromatin fractionation and cytochemistry detecting EGFP. Western blot analysis showed 42-kDa (DPPA4) and 75-kDa (DPPA4-EGFP) bands in ES cells transfected with DPPA4-EGFP expression vector, and the latter was not detected in mock-transfected cells (Fig. 1A). We carried out chromatin fractionation by increasing salt concentration. In the presence of 150 mM NaCl, DPPA4-EGFP, DPPA4, and core histone H3 were hardly solubilized, while a linker histone H1 was slightly solubilized (Fig. 1B). By addition of 500 mM NaCl, DPPA4-EGFP, DPPA4, and histone H1 were mostly solubilized, whereas histone H3 was retained in chromatin even under high-salt conditions (Fig. 1B). This suggests that DPPA4 is a chromatin factor showing a similar behavior to linker histone H1, but not core histone H3. DPPA4-EGFP, as well as endogenous DPPA4, localizing in chromatin during both the interphase and mitotic phase (Fig. 1D and F), suggesting that the localization of DPPA4-EGFP in ES cells corresponds to that of endogenous DPPA4. Taken together, these data suggest that DPPA4 is a chromatin factor like histone H1 rather than core histones.

Using ES cells transiently transfected with DPPA4-EGFP, linker histone $H1^0$-EGFP, and core histone H3-EGFP expression vectors, FRAP analysis was performed. In ES cells expressing histone H3-EGFP, fluorescence of bleaching strip was hardly recovered 120 s after bleaching, indicating that histone H3 is actually an immobile protein (Fig. 2A). In contrast, in ES cells expressing histone $H1^0$-EGFP or DPPA4-EGFP, fluorescence of bleaching strip gradually

© 2010 The Authors
Journal compilation © 2010 by the Molecular Biology Society of Japan/Blackwell Publishing Ltd.

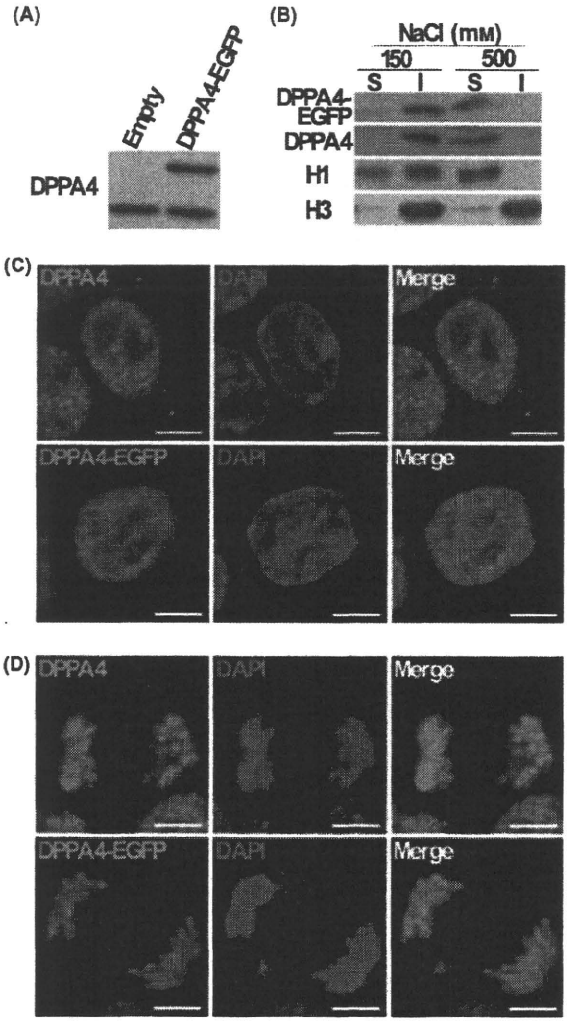

Figure 1 Cellular localization of developmental pluripotency associated 4 (DPPA4)-EGFP in embryonic stem (ES) cells. (A) Western blot analysis of DPPA4-EGFP expression in chromatin fraction of ES cells transfected with DPPA4-EGFP or empty vector. (B) Western blot analysis for DPPA4-EGFP, endogenous DPPA4, histone H1 and H3 in soluble (S) and insoluble (I) fractions of ES cells treated with the buffer containing 150 mM and 500 mM NaCl. (C-D) Confocal images of interphase (C) or metaphase (D) ES cells, showing endogenous DPPA4 immunostained with anti-DPPA4 antibodies (green; upper) and fluorescent DPPA4-EGFP (green; lower). Nuclei were counterstained with 4′,6′-diamino-2-phenylindole (DAPI, blue). Scale bars, 5 μm.

recovered within 120 s, indicating that DPPA4 and histone $H1^0$ are mobile proteins compared with histone H3. The time-dependent changes in fluorescence intensity of the bleaching strip in these cells were plotted versus the pre-bleach level to produce FRAP recovery curves. The histone H3 signal scarcely recovered (Fig. 2B), whereas DPPA4 and histone H1 showed gradual recovery after bleaching (Fig. 2C,D). Interestingly, FRAP recovery curves merged with DPPA4-EGFP, and histone $H1^0$-EGFP showed that the mobility of DPPA4 is very similar to that of histone $H1^0$ mobility in living ES cells (Fig. 2E).

DPPA4 directly binds to DNA *in vitro*

Next, to investigate the biochemical function of DPPA4, we purified recombinant DPPA4-His_6 protein expressed in *E. coli* (Fig. 3A). With the use of purified DPPA4, gel shift assay was performed to examine whether DPPA4 directly binds to DNA. Purified DPPA4 and pBluescript DNA were mixed and the protein-DNA complex was analyzed by agarose gel electrophoresis. As shown in Fig. 3B, the bands were stepwise shifted in a DPPA4 amount-dependent manner. These results are consistent with the previous report that DPPA4 has the SAP DNA-binding domain (Aravind & Koonin 2000). Stella/DPPA3, which has the SAP domain, binds to methylated DNA *in vitro* and protects against DNA demethylation in early mouse embryo (Nakamura *et al.* 2007). To investigate the effect of DNA methylation on the DNA-binding capacity of DPPA4, CpG sites of plasmid DNA were methylated by the CpG methylase *Sss* I. Methylated plasmid DNA showed resistance to digestion of *Hap II*, a methylation sensitive restriction enzyme (data not shown). Gel shift assay showed that DPPA4 binds to methylated plasmid DNA as well as non-methylated plasmid DNA (Fig. 3C), suggesting that DNA methylation does not affect DNA binding of DPPA4.

DPPA4 directly binds to histone H3 *in vitro* and *in vivo*

DPPA4 is considered a chromatin factor, providing the possibility of the association between DPPA4 and core histones. To examine whether DPPA4 directly binds to core histone proteins (H2A, H2B, H3 and H4) *in vitro*, we carried out Far-Western blotting analysis. Core histone proteins were purified from ES cells (Fig. 4A), and were used as a prey protein in Far-Western blotting analysis with purified DPPA4. As shown in Fig. 4B, histone H3 and H2B were detected, but neither H2A nor H4 bands. In case of using DPPA4 as a prey protein, the DPPA4 band was

© 2010 The Authors
Journal compilation © 2010 by the Molecular Biology Society of Japan/Blackwell Publishing Ltd.

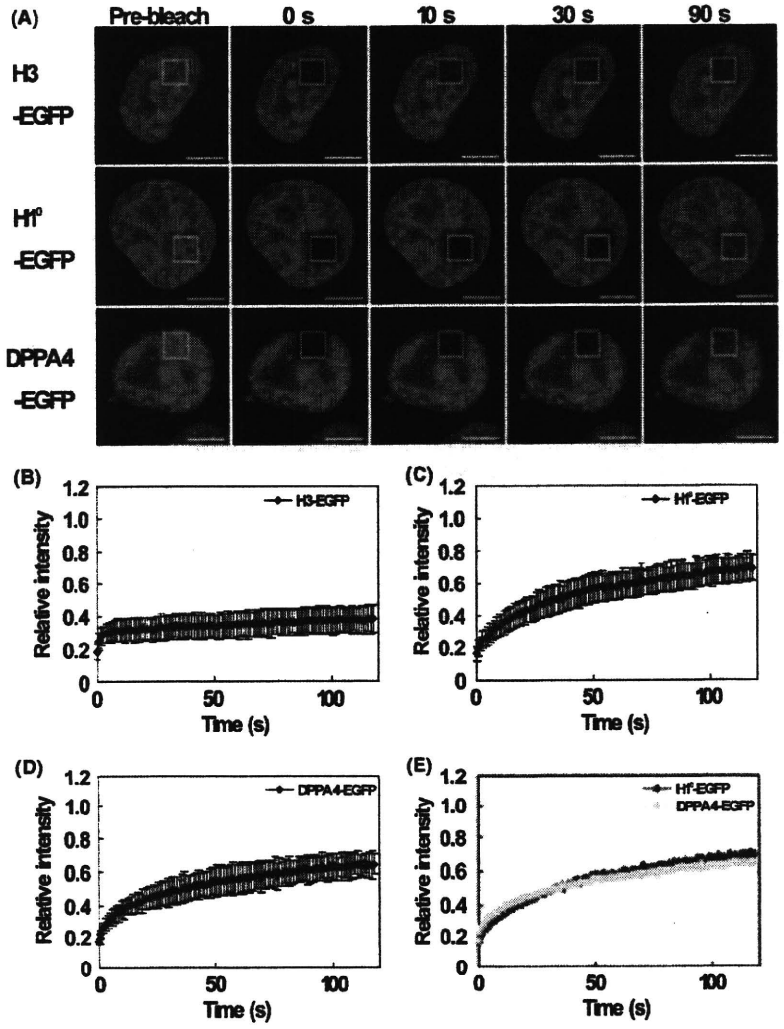

Figure 2 Fluorescence recovery after photobleaching (FRAP) analysis of developmental pluripotency associated 4 (DPPA4)-EGFP, histone $H1^0$-EGFP, and H3-EGFP in embryonic stem (ES) cells. (A) Representative images of FRAP analysis in living ES cells transfected with histone H3-EGFP, $H1^0$-EGFP, or DPPA4-EGFP expression vector. The bleach areas are marked with white squares. The fluorescence recovery was monitored and shown at indicated time points after bleaching. Scale bars, 5 μm. (B–D) Quantitative FRAP analysis (FRAP recovery curves) of transiently expressed histone H3-EGFP (B), $H1^0$-EGFP (C), and DPPA4-EGFP (D) in ES cells. Each value is the mean ± SD. (E) Comparison of FRAP recovery curves between ES cells expressing histone $H1^0$-EGFP (blue) and DPPA4-EGFP (yellow).

detected in a reciprocal experiment with histone H3 (data not shown). These data suggest that DPPA4 binds to histone H3 and H2B *in vitro*. To confirm DPPA4 binding to core histones, we performed *in vitro* co-immunoprecipitation using purified recombinant DPPA4 and core histone proteins with anti-DPPA4 antibodies. In the presence of histone H3 and H4, histone H3 was co-immunoprecipitated with anti-DPPA4 antibodies, but not with non-immune IgG (Fig. 4C). These results suggest direct binding between DPPA4 and histone H3 *in vitro*.

To investigate whether DPPA4 directly binds to core histone proteins in ES cells, co-immunoprecipitation between DPPA4 and core histones was performed using ES cell extracts. Whole ES cell extracts were sonicated to disrupt the nucleosome structure, and used for immunoprecipitation assay. DPPA4 was immunoprecipitated with histone H3 in ES cells,

© 2010 The Authors
Journal compilation © 2010 by the Molecular Biology Society of Japan/Blackwell Publishing Ltd.

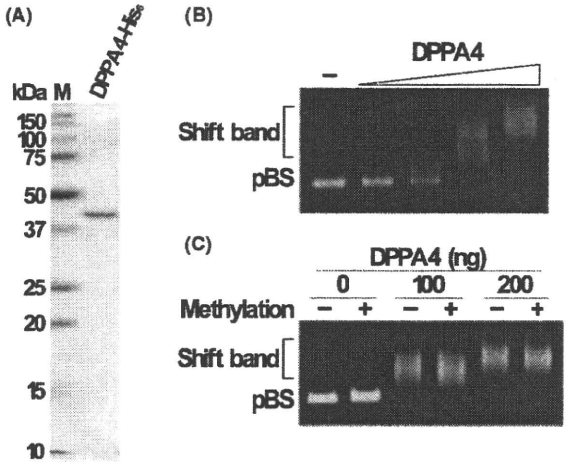

Figure 3 Gel shift analysis using developmental pluripotency associated 4 (DPPA4)-His_6. (A) Coomassie brilliant blue staining of the purified recombinant DPPA4-His_6 protein from *E. coli*. M, molecular mass markers. (B) Gel shift assay with plasmid DNA (pBlueScript II SK+; pBS) and increasing amount of DPPA4-His_6, (0, 100, 200, 400, and 800 ng). (C) Gel shift assay with methylated or non-methylated plasmid DNA (pBS) and increasing amount of recombinant DPPA4-His_6 (0, 100, and 200 ng).

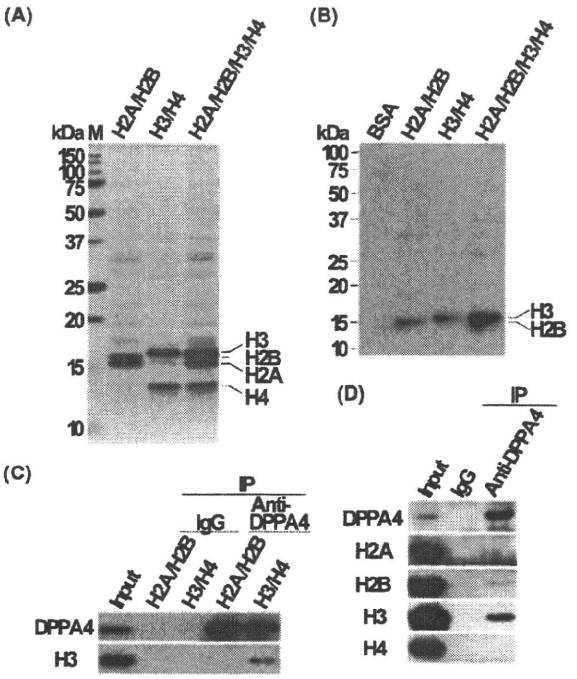

Figure 4 Interaction between developmental pluripotency associated 4 (DPPA4) and core histones *in vitro* and *in vivo*. (A) Coomassie brilliant blue staining of purified H2A/H2B, H3/H4, and H2A/H2B/H3/H4 from embryonic stem (ES) cells. M, molecular mass markers. (B) Far western blotting analysis using recombinant DPPA4-His_6 and purified histones as a bait- and prey protein, respectively. The bands were detected with anti-DPPA4 antibodies. Numbers on the left side of the gel indicate the position of marker proteins. (C) Western blot analysis of *in vitro* co-immunoprecipitation (IP) using purified core histones (H2A + H2B, H3 + H4) and recombinant DPPA4-His_6 by anti-DPPA4 antibodies or control IgG. The bands in input and IPs were detected with anti-DPPA4 or anti-H3 antibodies. (D) Western blot analysis of co-immunoprecipitation (IP) by anti-DPPA4 antibodies or control IgG with ES cell extracts. The bands in input and IPs were detected with anti-DPPA4, anti-H2A, anti-H2B, anti-H3, and anti-H4 antibodies.

whereas H2B was only slightly detected, and the others were not (Fig. 4D). These data suggest that DPPA4 is mainly associated with histone H3 in ES cells.

DPPA4 binds to DNA via the N-terminal region and to histone H3 via the C-terminal region

Next, to determine the DPPA4 regions mediating interactions with DNA and histone H3, we purified two truncated proteins, DPPA4 N-terminal region (DPPA4ΔC-His_6) containing the SAP domain and C-terminal region (DPPA4ΔN-His_6) (Fig. 5A,B). Using purified wild-type (wt) DPPA4 and truncated proteins, gel shift assay was performed. In the presence of DPPA4ΔC as well as wt DPPA4, the bands were stepwise shifted in a protein amount-dependent manner, whereas the bands were slightly shifted in the presence of DPPA4ΔN (Fig. 5C). These results suggest that the N-terminal region of DPPA4 has a greater binding affinity for DNA than the C-terminal region.

Likewise, we performed *in vitro* immunoprecipitation using these truncated proteins and total core histones with anti-6xHis antibodies. Histone H3 was efficiently precipitated with DPPA4ΔN compared with DPPA4 wt and DPPA4ΔC (Fig. 5D), indicating that the binding affinity of the C-terminal region of DPPA4 for histone H3 is higher than that of the N-terminal region. Taken together, these results suggest that DPPA4 associates with DNA and histone H3 via the N- and C-terminal regions, respectively.

DPPA4 modulates chromatin structure *in vitro*

Because a similar mobility of DPPA4 to linker histone $H1^0$ and DPPA4 binding to both DNA and

© 2010 The Authors
Journal compilation © 2010 by the Molecular Biology Society of Japan/Blackwell Publishing Ltd.

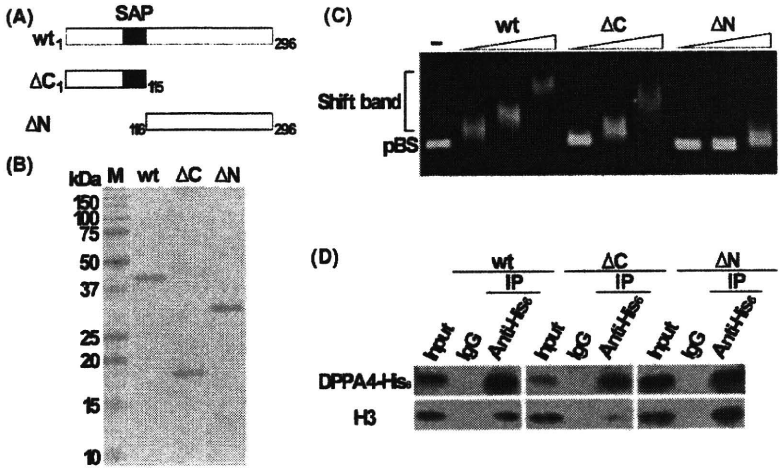

Figure 5 Binding analysis of truncated developmental pluripotency associated 4 (DPPA4) proteins to DNA or histone H3 *in vitro*. (A) Schematic representation of wild-type (wt) and truncated DPPA4 proteins (ΔC, ΔN). The SAP domain (amino acids 81-115) is depicted by the black box. (B) Coomassie brilliant blue staining of the purified recombinant wt DPPA4-His_6, DPPA4ΔC-His_6, and DPPA4ΔN-His_6 proteins from *E. coli*. M, molecular mass markers. (C) Gel shift assay with plasmid DNA (pBS) and increasing amount of DPPA4-His_6, DPPA4ΔC-His_6, or DPPA4ΔN-His_6 (100, 200, and 400 ng). (D) Western blot analysis of *in vitro* co-immunoprecipitation (IP) using purified H2A/H2B/H3/H4 and DPPA4-His_6, DPPA4ΔC-His_6, or DPPA4ΔN-His_6 by anti-His_6 antibodies or control IgG. The bands in input and IPs were detected with anti-6xHis (DPPA4) and anti-H3 antibodies (H3).

histone H3 were revealed, we hypothesized that DPPA4 modulates the chromatin structure like histone H1. Thus, we investigated whether the chromatin structure is affected by DPPA4 using *in vitro* reconstituted chromatin. *In vitro* reconstituted chromatin was incubated with purified histone $H1^0$ and DPPA4 (Fig. 6A), followed by digestion with MNase. The addition of histone $H1^0$ enhanced the resistance to MNase digestion compared to the addition of BSA (Fig. 6B), as previously reported (Kim *et al.* 2004). Similar to histone H1, the addition of DPPA4-His_6 resulted in an increase in the resistance to MNase digestion (Fig. 6B). These results indicate that DPPA4 incorporated into the reconstituted chromatin promoted the formation of nuclease-resistant chromatin structure like histone H1 and imply that DPPA4 modulates the chromatin structure in ES cells.

We further investigated whether the formation of nuclease-resistant chromatin structure requires DPPA4 binding to either DNA, histone H3 or both DNA and H3, using truncated DPPA4 proteins (Fig. 5A,B). The addition of DPPA4ΔC or DPPA4ΔN resulted in a decrease in the resistance to MNase digestion compared with wt DPPA4 (Fig. 6C). These results suggest that the DPPA4 binding to both DNA and histone H3 is required for the formation of nuclease-resistant chromatin structure.

Binding to both DNA and histone H3 is required for the proper dynamics of DPPA4 in ES cells

Finally, to investigate whether binding of DPPA4 to DNA and histone H3 affects the localization and mobility of DPPA4 in ES cells, we performed localization and FRAP analyses using truncated DPPA4-EGFP fusion proteins. The localization of truncated DPPA4-EGFP fusion proteins was compared with that of wt DPPA4 in ES cells. Confocal microscopy showed nuclear localization of DPPA4ΔC-EGFP and DPPA4ΔN-EGFP as well as DPPA4 wt-EGFP (Fig. 7A). DPPA4 wt-EGFP and DPPA4ΔN-EGFP were not localized in nucleoli, whereas DPPA4ΔC-EGFP was diffusely distributed in an entire nucleus (Fig. 7A).

In ES cells transiently transfected with DPPA4 wt-EGFP, DPPA4ΔC-EGFP, and DPPA4ΔN-EGFP expression vectors, FRAP analysis was performed. FRAP analysis showed that DPPA4ΔC-EGFP and DPPA4ΔN-EGFP signals were immediately recovered in contrast to the DPPA4 wt-EGFP signal (Fig. 7B–E). These data indicate that DPPA4 binding

© 2010 The Authors
Journal compilation © 2010 by the Molecular Biology Society of Japan/Blackwell Publishing Ltd.

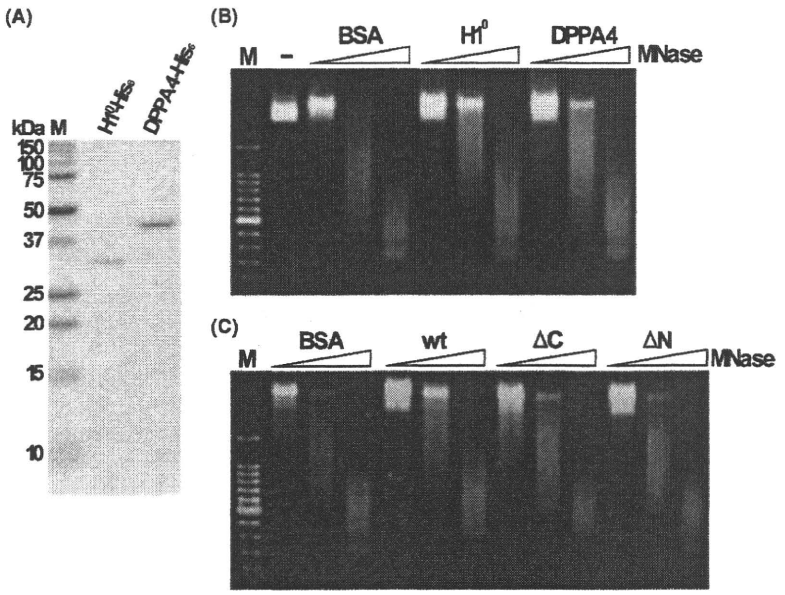

Figure 6 Modulation of chromatin structure by developmental pluripotency associated 4 (DPPA4). (A) Coomassie brilliant blue staining of the purified recombinant $H1^0$-His_6 and DPPA4-His_6 proteins from *E. coli*. M, molecular mass markers. (B) *In vitro* assembled chromatin with BSA, histone $H1^0$-His_6 ($H1^0$), or DPPA4-His_6 (DPPA4) was digested with increasing amount of MNase. (C) *In vitro* assembled chromatin with BSA, DPPA4-His_6 (wt), DPPA4ΔC-His_6 (ΔC), or DPPA4ΔN-His_6 (ΔN) was digested with increasing amount of MNase. Marker (M), 100-bp ladder.

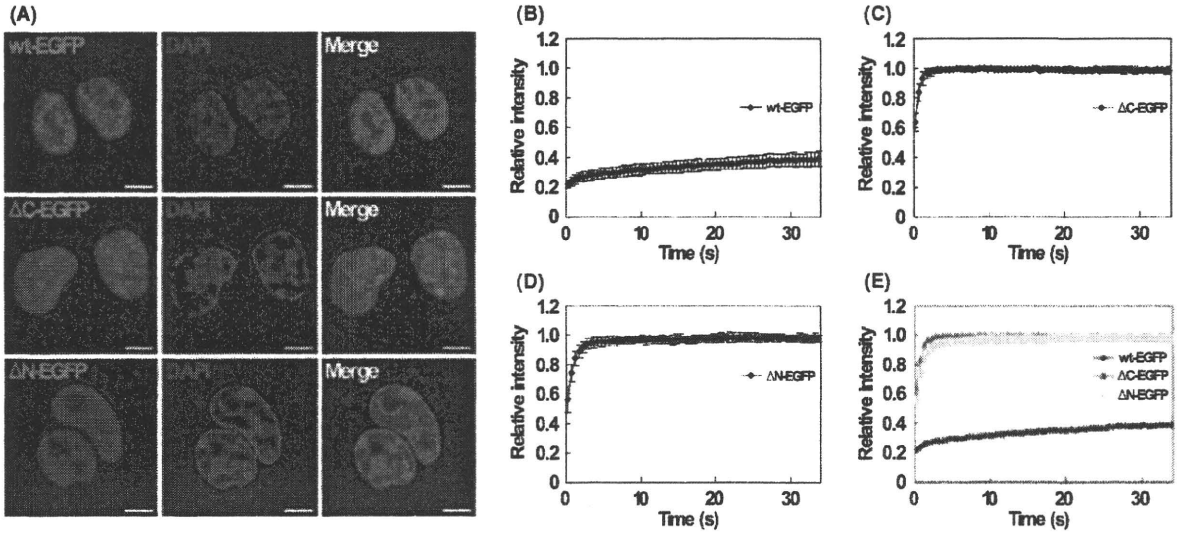

Figure 7 Cellular localization and fluorescence recovery after photobleaching (FRAP) analysis of truncated developmental pluripotency associated 4 (DPPA4) proteins in embryonic stem (ES) cells. (A) Confocal images of ES cells, showing fluorescent DPPA4-EGFP, DPPA4ΔC-EGFP, and DPPA4ΔN-EGFP (green). Nuclei were counterstained with DAPI (blue). Scale bars, 5 μm. (B-D) Quantitative FRAP analysis (FRAP recovery curves) in ES cells transiently expressing wt DPPA4-EGFP (B), DPPA4ΔC-EGFP (C), and DPPA4ΔN-EGFP (D). Each value is the mean ± SD. (E) Comparison of FRAP recovery curves between ES cells expressing DPPA4 wt-EGFP (red), DPPA4ΔC-EGFP (green), and DPPA4ΔN-EGFP (yellow).

© 2010 The Authors
Journal compilation © 2010 by the Molecular Biology Society of Japan/Blackwell Publishing Ltd.

to both DNA and histone H3 is required for the proper dynamics in ES cell chromatin.

Discussion

Some FRAP studies concerning ES cells have previously been reported: Meshorer *et al.* (2006) showed that architectural chromatin proteins such as linker histone H1 and heterochromatin protein 1 (HP1) loosely bind to chromatin; and van den Boom *et al.* (2007) revealed that undifferentiated embryonic cell transcription factor 1 (UTF1) is a strong chromatin-associated protein with a dynamic mobility similar to core histones. In the present study, we showed that the mobility of DPPA4 is different from that of core histones and similar to that of linker histone H1 in ES cells (Fig. 2). Previous studies have shown that histone H1 moves slowly compared with other chromatin binding factors such as HP1 and high-mobility-group (HMG) proteins (Phair *et al.* 2004), indicating that DPPA4, like histone H1, is a slow-moving mobile protein binding to chromatin. In addition, histone H1 is not a major global regulator of transcription, although histone H1 maintains the chromatin structure (Fan *et al.* 2005). Thus, it is predicted that DPPA4 is mainly involved in the maintenance of the genome-wide chromatin structure rather than overall transcriptional regulation, like histone H1. We also showed that the addition of DPPA4 enhances the resistance to MNase digestion (Fig. 6). It has been reported that histone H1 and poly(ADP-ribose) polymerase-1 (PARP-1) exert a similar effect on reconstituted chromatin as modulator of chromatin structure (Kim *et al.* 2004). Thus, it is likely that DPPA4 modulates the chromatin structure like histone H1 and PARP-1. Furthermore, DPPA4 is associated with DNA and core histone H3 (Figs 3 and 4), and it could not bind to histone H1 in our immunoprecipitation conditions (data not shown). Based on these results, we propose that DPPA4 modulates the chromatin structure via association with histone H3 and DNA in ES cells. We previously reported that DPPA4 plays an important role in the maintenance of pluripotency in association with active chromatin in ES cells (Masaki *et al.* 2007). Recently, it was suggested that the chromatin states of many inactive genes (so-called bivalent domains) are more permissive for transcription in ES cells than in differentiated cells (Spivakov & Fisher 2007). Taken together, DPPA4 is likely to contribute to the maintenance of these unique chromatin states in ES cells by modulating the chromatin structure in the permissive bivalent domain into a compact state. It has recently been reported that DPPA4 interacts with ES cell chromatin-remodeling complex es-BAF (Brg/Brahma-associated factors) required for pluripotency in ES cells (Ho *et al.* 2009). In addition, the chromatin-remodeling factor Chd1 required for pluripotency regulates the unique open chromatin structure of ES cell (Gaspar-Maia *et al.* 2009). These reports raise another possibility that DPPA4 is involved in chromatin remodeling and maintenance of the open chromatin structure in ES cells. Further studies are necessary to determine whether DPPA4 is involved in modulating the chromatin structure into the compact or open state in ES cells.

The analysis with truncated DPPA4 proteins revealed that the N-terminal region of DPPA4 including the SAP domain has an affinity to DNA, whereas the C-terminal region has a higher affinity to histone H3 than the N-terminal region (Fig. 5). Dppa2/4 conserved region included in the C-terminal region of DPPA4 (Siegel *et al.* 2009) seems to play an important role in association with histone H3. Both truncated DPPA4 proteins showed a weak effect on resistance to MNase digestion compared with wt DPPA4 (Fig. 6), allowing us to consider a possibility that the N-terminal and C-terminal regions of DPPA4 coordinately contribute to the proper formation of chromatin structure. In addition, N-terminal and C-terminal regions are essential for the proper mobility of DPPA4 in ES cells (Fig. 7). These analyses with truncated proteins support our model that DPPA4 modulates the chromatin structure in association with DNA and histone H3.

In our previous report, we suggested that DPPA4 associated with active chromatin contributes to the maintenance of pluripotency in ES cells without feeder cells (Masaki *et al.* 2007). However, it has been recently reported that DPPA4-deficient ES cells normally proliferate in the undifferentiated state on feeder cells (Madan *et al.* 2009). It is difficult to explain rationally the difference between our and their reports; there might be a difference between knockdown of DPPA4 expression and knockout of the gene, or a difference in culture conditions. Alternatively, DPPA4-deficient ES cells are more likely to lead to differentiation. However, the underlying common question is the actual role of DPPA4 in ES cells. In the present study, we investigated the behavior of DPPA4 focusing on the biochemical function of DPPA4 as a chromatin factor, and showed that DPPA4 has a similar mobility to linker histone H1, and directly interacts with DNA and histone H3 via the N- and C-terminal regions, respectively. Moreover, the chromatin

© 2010 The Authors
Journal compilation © 2010 by the Molecular Biology Society of Japan/Blackwell Publishing Ltd.

containing DPPA4 was resistant to MNase digestion when compared to that without DPPA4. These findings imply that DPPA4 modulates the chromatin structure in ES cells and raises the possibility that DPPA4 is involved in the maintenance of unique chromatin states of ES cell. Thus, elucidating the function of DPPA4 potentially facilitates revealing novel properties of unique chromatin states of ES cells.

Experimental procedures

ES cell culture

The mouse ES cell line, MGZRTcH2 (Masui *et al.* 2005), was maintained in ES medium consisting of Knockout DMEM (Gibco Life Technologies, Carlsbad, CA, USA) containing 1% embryonic stem cell screened fetal bovine serum (FBS; Hyclone Thermo Fisher Scientific, Waltham, MA, USA), 10% Knockout Serum Replacement (KSR), 2 mM L-glutamine, 100 U/mL penicillin, 100 μg/mL streptomycin, 100 μM MEM non-essential amino acids solution (Gibco Life Technologies), 0.3 mM monothioglycerol (Sigma-Aldrich, St. Louis, MO, USA), and 1000 U/mL LIF (Millipore, Billerica, MA, USA) on gelatin-coated dishes.

Immunocytochemistry and Western blotting

Immunocytochemistry and Western blotting were performed as described (Masaki *et al.* 2007). The following primary antibodies were used: DPPA4 (Masaki *et al.* 2007); GFP (GF090R; Nacalai Tesque, Kyoto, Japan); histone H1 (AE-4; Santa Cruz Biotechnology, Santa Cruz, CA, USA); histone H2A (Active Motif, Carlsbad, CA, USA); histone H2B (Active Motif); histone H3 (ab1791, Abcam, Cambridge, UK); histone H4 (Active Motif); β-actin (AC-74, Sigma); and 6xHis (A190-114A, BETHYL Laboratories, Montgomery, USA).

FRAP analysis

The mouse DPPA4, DPPA4ΔC (1-348), DPPA4ΔN (349-888), histone $H1^0$, and histone H3 cDNAs were subcloned into pBlueScript II SK+ (pBS) vector (Stratagene Agilent Technologies, Santa Clara, CA, USA). Each cDNA in the plasmid was excised and ligated into EGFP fusion protein expression vector, pEGFP-N1 (Clontech Takara Bio, Shiga, Japan). These vectors were transfected into ES cells with lipofectamine2000 (Invitrogen Life Technologies, Carlsbad, CA, USA), and transfected ES cells were plated on gelatin-coated glass bottom dishes (Matsunami, Osaka, Japan) 24 h after transfection. The next day, the culture medium was changed to ES cell medium containing Leibovitz L-15 medium (Gibco Life Technologies) instead of Knockout DMEM. FRAP experiments were performed with a LSM 510 META confocal microscope (Carl Zeiss, Oberkochen, Germany). The pre-bleach image was collected, followed by a 500-ms bleach pulse with a spot 4 μm in diameter. Bleaching was performed with the 488-nm line of a 25 mW argon laser set to 100%. Single images were collected with the 488-nm line of the argon laser (set to 5%) every 1 s for 120 s. FRAP recovery curves were created from images with the background subtracted. Total fluorescence was determined for each image and compared to the total pre-bleach fluorescence to determine the amount of fluorescence lost during the imaging. The fluorescence intensity in the bleached area was normalized to the initial fluorescence in the bleached area.

Preparation and purification of proteins

Subcloned cDNAs of mouse DPPA4, DPPA4ΔC, DPPA4ΔN, and histone $H1^0$ were inserted into pET21a+ (Novagen Merck, Darmstadt, Germany). *E. coli* BL21(DE3) cells were transformed with each vector, and protein expression was induced by 100 μM isopropyl beta-D-1-thiogalactopyranoside at 30 °C for 2 h. The cells were treated with lysis buffer [20 mM Tris-HCl, 500 mM NaCl, 1% NP-40, 1 mg/mL lysozyme, 5% glycerol, and protease inhibitor cocktail (PIC; Roche Diagnostic, Basel, Switzerland)] and sonicated. The whole extract was centrifuged at 15 000 g for 30 min. Using supernatant, recombinant proteins were purified by TALON metal affinity resin (Clontech Takara Bio) according to the manufacturer's instructions. Core histone proteins were purified from mouse ES cells by histone purification kit (Active Motif) according to the manufacturer's instructions. The purity of these proteins was confirmed by SDS-PAGE and coomassie brilliant blue staining.

Gel shift assay

pBS plasmid DNA (100 ng) was incubated with 100, 200, 400, or 800 ng purified DPPA4-His_6, DPPA4ΔC-His_6, or DPPA4ΔN-His_6 proteins on ice for 30 min in 60 mM NaCl, 50 mM $NaHPO_4$, 2 mM EDTA, 10% glycerol, and 2 mg/mL BSA. The samples were electrophoresed on a 1% agarose gel, and the DNA visualized by ethidium bromide staining. To obtain methylated pBS plasmid DNA, CpG methylase (*Sss* I Methylase; New England Biolabs, Ipswich, MA, USA) was used.

Far-Western blot analysis

Far-Western blotting was carried out as described by Wu *et al.* 2007. Briefly, 250 ng of each purified core histone was separated by SDS-PAGE and transferred to a nitrocellulose membrane. Proteins on the membrane were denatured and renatured by gradually reducing the guanidine-HCl concentration. After blocking with 5% non-fat dry milk, the membrane was incubated with purified DPPA4-His_6 (500 ng/mL) in blocking reagent followed by detection with anti-DPPA4 antibodies.

© 2010 The Authors
Journal compilation © 2010 by the Molecular Biology Society of Japan/Blackwell Publishing Ltd.

Co-immunoprecipitation

ES cells were washed with PBS, resuspended in buffer C (20 mM Tris-HCl, 150 mM NaCl, 2 mM EDTA, 0.1% Tween20, and PIC), and incubated on ice for 20 min. The lysate was robustly sonicated and centrifuged for 30 min at 16 000 g. The supernatant was incubated overnight with anti-DPPA4 antibodies or control IgG (10 μg), and then incubated with protein G Sepharose (GE Healthcare, Waukesha, WI, USA) for 1 h at 4 °C. The beads were washed three times with buffer B (20 mM Tris-HCl, 150 mM NaCl, 0.1% Tween20, 0.5 mM EDTA, 10% glycerol, and PIC) followed by boiling with SDS sample buffer (50 mM Tris-HCl, pH 6.8, 2% SDS, 10% glycerol, 2% 2-mercaptoethanol, and 0.2% bromphenolblue). For *in vitro* co-immunoprecipitation, purified histone H2A + H2B (5 μg), histone H3 + H4 (5 μg) or total core histones (10 μg) and recombinant DPPA4-His_6 (1.5 μg), DPPA4ΔC-His_6 or DPPA4ΔN-His_6 (equimolar amount to DPPA4-His_6) proteins were incubated in buffer B for 1 h at 4 °C. Anti-DPPA4 antibodies or control IgG (10 μg) were added to each mixture followed by overnight incubation. The mixtures were then incubated with protein G Sepharose beads blocked with 5% non-fat dry milk for 1 h at 4 °C. The beads were washed three times with buffer B and boiled in SDS sample buffer. These samples were subjected to SDS-PAGE and Western blot analysis using rabbit TrueBlot (eBioscience, San Diego, CA, USA) as secondary antibodies.

Chromatin reconstitution

In vitro reconstituted chromatin was prepared by using mouse ES cell core histones, pBS plasmid DNA, and chromatin assembly kit (Active Motif) according to the manufacturer's instructions. Subsequent to chromatin assembly, either DPPA4-His_6, DPPA4ΔC-His_6, DPPA4ΔN-His_6, $H1^0$-His_6 or BSA was added to the reconstituted chromatin at a ratio of one molecule per nucleosome, and the chromatin mixtures were incubated for 1 h at 27 °C. The chromatin mixtures were digested with several concentrations of enzymatic shearing cocktail containing MNase (chromatin assembly kit) for 5 min, subsequently EDTA and proteinase K (Sigma-Aldrich) were added to the mixtures to stop digestion, and incubated overnight. The mixtures were electrophoresed on a 1.5% agarose gel, and the DNA was visualized by ethidium bromide.

Acknowledgement

This work was supported in part by Grants-in-Aid from Japan Society for the Promotion of Science for JSPS Fellows and for Exploratory Research (20659047).

References

Aravind, L. & Koonin, E.V. (2000) SAP - a putative DNA-binding motif involved in chromosomal organization. *Trends Biochem. Sci.* **25**, 112–114.

Azuara, V., Perry, P., Sauer, S., Spivakov, M., Jørgensen, H.F., John, R.M., Gouti, M., Casanova, M., Warnes, G., Merkenschlager, M. & Fisher, A.G. (2006) Chromatin signatures of pluripotent cell lines. *Nat. Cell Biol.* **8**, 532–538.

Bernstein, B.E., Mikkelsen, T.S., Xie, X., Kamal, M., Huebert, D.J., Cuff, J., Fry, B., Meissner, A., Wernig, M., Plath, K., Jaenisch, R., Wagschal, A., Feil, R., Schreiber, S.L. & Lander, E.S. (2006) A bivalent chromatin structure marks key developmental genes in embryonic stem cells. *Cell* **125**, 315–326.

Boiani, M. & Schöler, H.R. (2005) Regulatory networks in embryo-derived pluripotent stem cells. *Nat. Rev. Mol. Cell Biol.* **6**, 872–884.

van den Boom, V., Kooistra, S.M., Boesjes, M., Geverts, B., Houtsmuller, A.B., Monzen, K., Komuro, I., Essers, J., Drenth-Diephuis, L.J. & Eggen, B.J. (2007) UTF1 is a chromatin-associated protein involved in ES cell differentiation. *J. Cell Biol.* **178**, 913–924.

Bortvin, A., Eggan, K., Skaletsky, H., Akutsu, H., Berry, D.L., Yanagimachi, R., Page, D.C. & Jaenisch, R. (2003) Incomplete reactivation of Oct4-related genes in mouse embryos cloned from somatic nuclei. *Development* **130**, 1673–1680.

Boyer, L.A., Lee, T.I., Cole, M.F., Johnstone, S.E., Levine, S.S., Zucker, J.P., Guenther, M.G., Kumar, R.M., Murray, H.L., Jenner, R.G., Gifford, D.K., Melton, D.A., Jaenisch, R. & Young, R.A. (2005) Core transcriptional regulatory circuitry in human embryonic stem cells. *Cell* **122**, 947–956.

Boyer, L.A., Plath, K., Zeitlinger, J., *et al.* (2006) Polycomb complexes repress developmental regulators in murine embryonic stem cells. *Nature* **441**, 349–353.

Burdon, T., Smith, A. & Savatier, P. (2002) Signaling, cell cycle and pluripotency in embryonic stem cells. *Trends Cell Biol.* **12**, 432–438.

Chakravarthy, H., Boer, B., Desler, M., Mallanna, S.K., McKeithan, T.W. & Rizzino, A. (2008) Identification of DPPA4 and other genes as putative Sox2:Oct-3/4 target genes using a combination of in silico analysis and transcription-based assays. *J. Cell. Physiol.* **216**, 651–662.

Chambers, I., Colby, D., Robertson, M., Nichols, J., Lee, S., Tweedie, S. & Smith, A. (2003) Functional expression cloning of Nanog, a pluripotency sustaining factor in embryonic stem cells. *Cell* **113**, 643–655.

Fan, Y., Nikitina, T., Zhao, J., Fleury, T.J., Bhattacharyya, R., Bouhassira, E.E., Stein, A., Woodcock, C.L. & Skoultchi, A.I. (2005) Histone H1 depletion in mammals alters global chromatin structure but causes specific changes in gene regulation. *Cell* **123**, 1199–1212.

Gaspar-Maia, A., Alajem, A., Polesso, F., Sridharan, R., Mason, M.J., Heidersbach, A., Ramalho-Santos, J., McManus, M.T., Plath, K., Meshorer, E. & Ramalho-Santos, M. (2009) Chd1 regulates open chromatin and pluripotency of embryonic stem cells. *Nature* **460**, 863–868.

Hamatani, T., Carter, M.G., Sharov, A.A. & Ko, M.S. (2004) Dynamics of global gene expression changes during mouse preimplantation development. *Dev. Cell* **6**, 117–131.

© 2010 The Authors
Journal compilation © 2010 by the Molecular Biology Society of Japan/Blackwell Publishing Ltd.

Ho, L., Ronan, J.L., Wu, J., Staahl, B.T., Chen, L., Kuo, A., Lessard, J., Nesvizhskii, A.I., Ranish, J. & Crabtree, G.R. (2009) An embryonic stem cell chromatin remodeling complex, esBAF, is essential for embryonic stem cell self-renewal and pluripotency. *Proc. Natl Acad. Sci. USA* **106**, 5181–5186.

Ivanova, N., Dobrin, R., Lu, R., Kotenko, I., Levorse, J., DeCoste, C., Schafer, X., Lun, Y. & Lemischka, I.R. (2006) Dissecting self-renewal in stem cells with RNA interference. *Nature* **442**, 533–538.

Jiang, J., Chan, Y.S., Loh, Y.H., Cai, J., Tong, G.Q., Lim, C.A., Robson, P., Zhong, S. & Ng, H.H. (2008) A core Klf circuitry regulates self-renewal of embryonic stem cells. *Nat. Cell Biol.* **10**, 353–360.

Keller, G. (2005) Embryonic stem cell differentiation: emergence of a new era in biology and medicine. *Genes Dev.* **19**, 1129–1155.

Kim, M.Y., Mauro, S., Gévry, N., Lis, J.T. & Kraus, W.L. (2004) NAD^+-dependent modulation of chromatin structure and transcription by nucleosome binding properties of PARP-1. *Cell* **119**, 803–814.

Lee, T.I., Jenner, R.G., Boyer, L.A., *et al.* (2006) Control of developmental regulators by Polycomb in human embryonic stem cells. *Cell* **125**, 301–313.

Madan, B., Madan, V., Weber, O., Tropel, P., Blum, C., Kieffer, E., Viville, S. & Fehling, H.J. (2009) The pluripotency-associated gene Dppa4 is dispensable for embryonic stem cell identity and germ cell development but essential for embryogenesis. *Mol. Cell. Biol.* **29**, 3186–3203.

Maldonado-Saldivia, J., van den Bergen, J., Krouskos, M., Gilchrist, M., Lee, C., Li, R., Sinclair, A.H., Surani, M.A. & Western, P.S. (2007) Dppa2 and Dppa4 are closely linked SAP motif genes restricted to pluripotent cells and the germ line. *Stem Cells* **25**, 19–28.

Masaki, H., Nishida, T., Kitajima, S., Asahina, K. & Teraoka, H. (2007) Developmental pluripotency-associated 4 (DPPA4) localized in active chromatin inhibits mouse embryonic stem cell differentiation into a primitive ectoderm lineage. *J. Biol. Chem.* **282**, 33034–33042.

Masui, S., Nakatake, Y., Toyooka, Y., Shimosato, D., Yagi, R., Takahashi, K., Okochi, H., Okuda, A., Matoba, R., Sharov, A.A., Ko, M.S. & Niwa, H. (2007) Pluripotency governed by Sox2 via regulation of Oct3/4 expression in mouse embryonic stem cells. *Nat. Cell Biol.* **9**, 625–635.

Masui, S., Shimosato, D., Toyooka, Y., Yagi, R., Takahashi, K. & Niwa, H. (2005) An efficient system to establish multiple embryonic stem cell lines carrying an inducible expression unit. *Nucleic Acids Res.* **33**, e43.

Meshorer, E., Yellajoshula, D., George, E., Scambler, P.J., Brown, D.T. & Misteli, T. (2006) Hyperdynamic plasticity of chromatin proteins in pluripotent embryonic stem cells. *Dev. Cell* **10**, 105–116.

Mitsui, K., Tokuzawa, Y., Itoh, H., Segawa, K., Murakami, M., Takahashi, K., Maruyama, M., Maeda, M. & Yamanaka, S. (2003) The homeoprotein Nanog is required for maintenance of pluripotency in mouse epiblast and ES cells. *Cell* **113**, 631–642.

Nakamura, T., Arai, Y., Umehara, H., Masuhara, M., Kimura, T., Taniguchi, H., Sekimoto, T., Ikawa, M., Yoneda, Y., Okabe, M., Tanaka, S., Shiota, K. & Nakano, T. (2007) PGC7/Stella protects against DNA demethylation in early embryogenesis. *Nat. Cell Biol.* **9**, 64–71.

Niwa, H., Ogawa, K., Shimosato, D. & Adachi, K. (2009) A parallel circuit of LIF signalling pathways maintains pluripotency of mouse ES cells. *Nature* **460**, 118–122.

Niwa, H., Toyooka, Y., Shimosato, D., Strumpf, D., Takahashi, K., Yagi, R. & Rossant, J. (2005) Interaction between Oct3/4 and Cdx2 determines trophectoderm differentiation. *Cell* **123**, 917–929.

Phair, R.D., Scaffidi, P., Elbi, C., Vecerová, J., Dey, A., Ozato, K., Brown, D.T., Hager, G., Bustin, M. & Misteli, T. (2004) Global nature of dynamic protein-chromatin interactions in vivo: three-dimensional genome scanning and dynamic interaction networks of chromatin proteins. *Mol. Cell. Biol.* **24**, 6393–6402.

Siegel, D., Schuff, M., Oswald, F., Cao, Y. & Knöchel, W. (2009) Functional dissection of XDppa2/4 structural domains in Xenopus development. *Mech. Dev.* **126**, 974–989.

Spivakov, M. & Fisher, A.G. (2007) Epigenetic signature of stem-cell identity. *Nat. Rev. Genet.* **8**, 263–271.

Szutorisz, H., Georgiou, A., Tora, L. & Dillon, N. (2006) The Proteasome restricts permissive transcription at tissue-specific gene loci in embryonic stem cells. *Cell* **127**, 1375–1388.

Takahashi, K., Tanabe, K., Ohnuki, M., Narita, M., Ichisaka, T., Tomoda, K. & Yamanaka, S. (2007) Induction of pluripotent stem cells from adult human fibroblasts by defined factors. *Cell* **131**, 861–872.

Thomson, J.A., Itskovitz-Eldor, J., Shapiro, S.S., Waknitz, M.A., Swiergiel, J.J., Marshall, V.S. & Jones, J.M. (1998) Embryonic stem cell lines derived from human blastocysts. *Science* **282**, 1145–1147.

Wu, Y., Li, Q. & Chen, X.Z. (2007) Detecting protein-protein interactions by far western blotting. *Nat. Protoc.* **2**, 3278–3284.

Yu, J., Vodyanik, M.A., Smuga-Otto, K., Antosiewicz-Bourget, J., Frane, J.L., Tian, S., Nie, J., Jonsdottir, G.A., Ruotti, V., Stewart, R., Slukvin, I.I. & Thomson, J.A. (2007) Induced pluripotent stem cell lines derived from human somatic cells. *Science* **318**, 1917–1920.

Zhang, J., Tam, W.L., Tong, G.Q., Wu, Q., Chan, H.Y., Soh, B.S., Lou, Y., Yang, J., Ma, Y., Chai, L., Ng, H.H., Lufkin, T., Robson, P. & Lim, B. (2006) Sall4 modulates embryonic stem cell pluripotency and early embryonic development by the transcriptional regulation of Pou5f1. *Nat. Cell Biol.* **8**, 1114–1123.

Received: 6 October 2009
Accepted: 23 December 2009

© 2010 The Authors
Journal compilation © 2010 by the Molecular Biology Society of Japan/Blackwell Publishing Ltd.

Supplemental Material can be found at:
http://www.jbc.org/content/suppl/2010/03/19/M110.101808.DC1.html

THE JOURNAL OF BIOLOGICAL CHEMISTRY VOL. 285, NO. 20, pp. 15201–15208, May 14, 2010
© 2010 by The American Society for Biochemistry and Molecular Biology, Inc. Printed in the U.S.A.

Transcription-dependent Activation of Ataxia Telangiectasia Mutated Prevents DNA-dependent Protein Kinase-mediated Cell Death in Response to Topoisomerase I Poison*[S]

Received for publication, January 6, 2010, and in revised form, March 18, 2010 Published, JBC Papers in Press, March 19, 2010, DOI 10.1074/jbc.M110.101808

Ryo Sakasai[‡1], Hirobumi Teraoka[‡], Masatoshi Takagi[§], and Randal S. Tibbetts[¶]

From the [‡]Department of Pathological Biochemistry, Medical Research Institute, Tokyo Medical and Dental University, Tokyo 101-0062, Japan, the [§]Department of Pediatrics and Developmental Biology, Tokyo Medical and Dental University, Tokyo 113-8519, Japan, and the [¶]Department of Pharmacology, University of Wisconsin School of Medicine and Public Health, Madison, Wisconsin 53706

Camptothecin (CPT) is a topoisomerase I inhibitor, derivatives of which are being used for cancer chemotherapy. CPT-induced DNA double-strand breaks (DSBs) are considered a major cause of its tumoricidal activity, and it has been shown that CPT induces DNA damage signaling through the phosphatidylinositol 3-kinase-related kinases, including ATM (ataxia telangiectasia mutated), ATR (ATM and Rad3-related), and DNA-PK (DNA-dependent protein kinase). In addition, CPT causes DNA strand breaks mediated by transcription, although the downstream signaling events are less well characterized. In this study, we show that CPT-induced activation of ATM requires transcription. Mechanistically, transcription inhibition suppressed CPT-dependent activation of ATM and blocked recruitment of the DNA damage mediator p53-binding protein 1 (53BP1) to DNA damage sites, whereas ATM inhibition abrogated CPT-induced G_1/S and S phase checkpoints. Functional inactivation of ATM resulted in DNA replication-dependent hyperactivation of DNA-PK in CPT-treated cells and dramatic CPT hypersensitivity. On the other hand, simultaneous inhibition of ATM and DNA-PK partially restored CPT resistance, suggesting that activation of DNA-PK is proapoptotic in the absence of ATM. Correspondingly, comet assay and cell cycle synchronization experiments suggested that transcription collapse occurring as the result of CPT treatment are converted to frank double-strand breaks when ATM-deficient cells bypass the G_1/S checkpoint. Thus, ATM suppresses DNA-PK-dependent cell death in response to topoisomerase poisons, a finding with potential clinical implications.

The topoisomerase I (TopI)[2] poison camptothecin (CPT) and its clinically relevant derivatives, topotecan and irinotecan, have been intensively studies for their tumoricidal properties. The molecular target of CPT is TopI, an enzyme that mediates the relaxation of supercoiled DNA (1). This is achieved through the transient introduction of a DNA single-strand break that permits the rotational relaxation of double-stranded DNA. The TopI reaction cycle involves the formation of a transient phosphotyrosyl bond between Tyr^{723} of the enzyme active site and a 3′ DNA end. CPT stabilizes covalent TopI-DNA cleavage complexes (TopI-cc), which are converted into DNA double-strand breaks (DSBs) upon encountering active DNA replication forks (1).

The signaling and repair of CPT-mediated damage have been the focus of intensive research. CPT-induced DSBs possess a single DNA double-strand end (DSE) that is generally not an efficient substrate for nonhomologous end joining DSB repair, which is mediated by DNA-dependent protein kinase (DNA-PK) composed of DNA-PKcs and Ku protein. Instead, CPT-induced DSEs are repaired by homologous recombination (HR) repair, which utilizes a sister chromatid and primes restart of the obstructed DNA replication fork (2, 3). CPT-induced DSEs strongly activate cell cycle checkpoint pathways downstream of the ATM (ataxia telangiectasia mutated) and ATR (ATM and Rad3-related) protein kinases. CPT-induced damage in S phase activates the ATR-Chk1 pathway that mediates S phase arrest (4). Consistent with these important S phase functions, ATR- or Chk1-deficient cells are exquisitely sensitive to TopI poisons (4, 5).

In addition to replication-mediated DNA damage, TopI-cc pose a block to processive RNA polymerase complexes, and the collision of RNA polymerase with TopI-cc results in transcription-mediated DNA damage (6). Although the mechanisms of transcription-coupled damage and signaling are not well understood, recent studies suggest a new role for the ATM protein kinase. CPT-induced activation of ATM is suppressed by inhibitors of transcription, and it has been proposed that ATM responds to RNA·DNA hybrid R-loops that form at stalled RNA polymerase II transcription bubbles (7). However, the detection and signaling of CPT-induced, transcription-dependent DNA damage are not well understood, nor is it clear

* This work was supported, in whole or in part, by National Institutes of Health Grant CA124722. This work was also supported by a grant from the American Cancer Society, a Shaw Scientist Award (to R. S. T.) from the Greater Milwaukee Foundation, and by Grant-in-aid 20659047 from Japan Society for the Promotion of Science for Exploratory Research (to H. T.).

[S] The on-line version of this article (available at http://www.jbc.org) contains supplemental Figs. S1–S5.

[1] To whom correspondence should be addressed: Dept. of Molecular Oncology, Graduate School of Medical Sciences, Kyushu University, Fukuoka 812-8582, Japan. E-mail: sakasai@surg2.med.kyushu-u.ac.jp.

[2] The abbreviations used are: TopI, topoisomerase I; TopI-cc, TopI cleavage complex; CPT, camptothecin; DSB, double-strand break; DSE, double-strand end; DNA-PK, DNA-dependent protein kinase; HR, homologous recombination; ATM, ataxia telangiectasia mutated; ATR, ATM and Rad3-related; DRB, 5,6-dichloro-1-β-D-ribofuranosylbenzimidazole; HU, hydroxyurea; siRNA, small interfering RNA; BrdUrd, bromodeoxyuridine; IR, ionizing radiation; 53BP1, p53-binding protein 1; RPA2, replication protein A2.

Downloaded from www.jbc.org at Tokyo Ikashika Daigaku, on February 27, 2011

whether transcription-mediated DNA damage contributes significantly to CPT cytotoxicity.

In this study, we investigated transcription-dependent and -independent pathways activated by CPT in human cells. We show that ATM is critically important for initiation of the G_1/S phase checkpoint in response to CPT and that transcription-dependent activation of ATM in G_1 phase suppresses DNA strand breakage leading to DNA-PK activation in S phase cells. These findings have implications for understanding CPT tumoricidal activity.

EXPERIMENTAL PROCEDURES

Cell Culture and Irradiation—HeLa, U2OS, and HCT116 cells were obtained from American Type Culture Collection and maintained in Dulbecco's modified Eagle's medium with 10% fetal bovine serum. SV40-transformed GM00637H (ATM+), GM05849C (ATM−), (obtained from Coriell Cell Repositories), and hTERT-immortalized SuSa/Tn (ATM+), AT1OS/Tn (ATM−) (kindly provided by Dr. K Ishizaki) (8) were cultured in Dulbecco's modified Eagle's medium with 10% fetal bovine serum. Cells were UV- and IR-irradiated as reported (9). CPT, VP-16, 5,6-dichloro-1-β-D-ribofuranosylbenzimidazole (DRB), KU-55933, NU7026, hydroxyurea (HU), and thymidine were purchased from Sigma. To knock down TopBP1 and RNF8 expression, siRNA SMART pool targeting each gene (Dharmacon) was used. siRNAs were transfected as described (10).

Antibodies and Immunofluorescence—Antibodies were obtained from following suppliers: Bethyl Laboratories (p53-binding protein 1 (53BP1), A300-272A), Oncogene (replication protein A (RPA), Ab-3; BrdUrd, Ab-2), Millipore (γH2AX, JBW301), Calbiochem (Rad51, PC130), Abcam (phospho-DNA-PKcs, ab18192, Chk2, ab8108), R&D Systems (phospho-ATM, AF-165; phospho-Chk1 Ser^{317}, AF-2054; phospho-Chk2, AF-1626), GeneTex (ATM, GTX70103), Thermo Scientific (DNA-PKcs, Ab-4), Cell Signaling Technology (phospho-Chk1 S345, no.2341), and Santa Cruz Biotechnology (Chk1, G-4). Cell preparation for staining of 53BP1, γH2AX and incorporated BrdUrd was performed as described (9). For RPA2 and Rad51 staining, cells were preextracted with phosphate-buffered saline containing 0.1% Triton X-100. The fixed cells were incubated with primary antibodies specific for 53BP1, BrdUrd, γH2AX, and Rad51. After incubation with secondary antibodies, cell nuclei were stained with 4′,6-diamidino-2-phenylindole (2 μg/ml). A Carl Zeiss Axiovert 200 fluorescence microscope or LSM510 laser-scanning microscope was used to visualize samples.

Western Blotting—Cell lysis, SDS-PAGE, and gel transfer were performed as described (9). After incubation with secondary antibody, the membranes were visualized using SuperSignal chemiluminescent substrate (Pierce).

Cell Cycle Synchronization and Flow Cytometry—To synchronize cells in the S phase, cells were treated with thymidine at 2.5 mM for 18 h and incubated with a fresh medium for 5 h. To collect G_1 phase cells, cells were treated with nocodazole for 12 h and released with a fresh medium for 5 h. For cell cycle analysis, cells were harvested and stained with propidium iodide after fixing with 70% ethanol. Propidium iodide-stained cells were analyzed using a FACSCalibur (BD Biosciences).

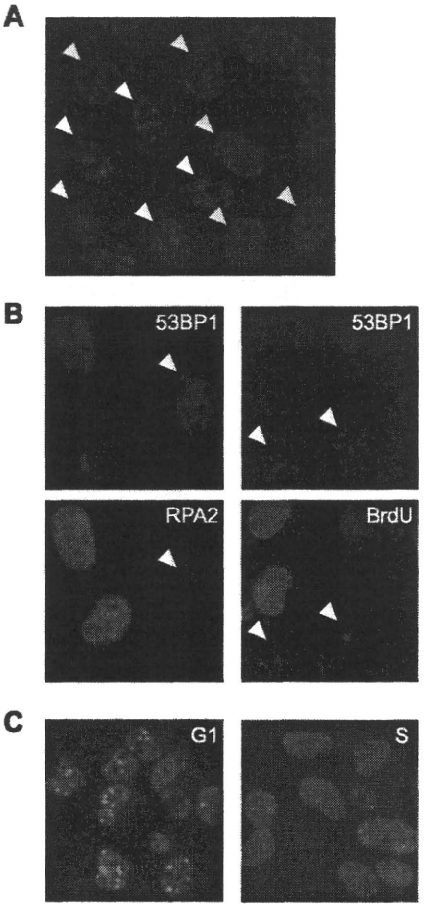

FIGURE 1. **CPT induces two distinct types of 53BP1 foci.** *A*, representative image of 53BP1 foci induced by CPT (2 μM, 1 h) treatment. The HeLa cells denoted by *white arrowheads* represent Type I 53BP1 foci, whereas *yellow arrowheads* denote Type II foci. *B*, Type I 53BP1 foci occurring in non-S phase cells. HeLa cells were treated with CPT (2 μM, 1 h) and stained with anti-53BP1 and RPA2 antibodies (*left*). To observe DNA synthesis, cells were treated with BrdUrd (20 μM, 20 min) and stained with α-53BP1 and α-BrdUrd antibodies (*right*). *C*, CPT-induced 53BP1 foci in G_1 or S phase cells. Cells were synchronized in G_1 phase and S phase by release from nocodazole block and thymidine block, respectively. After treatment with CPT (2 μM, 1 h), cells were stained with anti-53BP1 antibody.

Neutral Comet Assay—Cells were suspended in 0.7% low melting point agarose and spread on glass slides precoated with 1% agarose. Slides were overlaid with coverslips that were removed after the gel solidified. The gel was treated with lysis solution (Trevigen) for 30 min at 4 °C in the dark and electrophoresed at 1 V/cm for 17 min. Comet tails were stained with SYBR Green I (BMA) and analyzed by fluorescent microscope.

RESULTS

CPT Induces Two Types of 53BP1 Foci in Mammalian Cells—53BP1 is an adaptor protein that is recruited to nuclear foci in response to genotoxic stimuli, including ionizing radiation-induced DSBs and CPT-associated DSEs (11, 12). Following the treatment of HeLa cells with CPT, we observed two distinct 53BP1 localization patterns: Type I exhibited large 53BP1 foci that typically numbered fewer than 15/cell; Type II displayed

Downloaded from www.jbc.org at Tokyo Ikashika Daigaku, on February 27, 2011

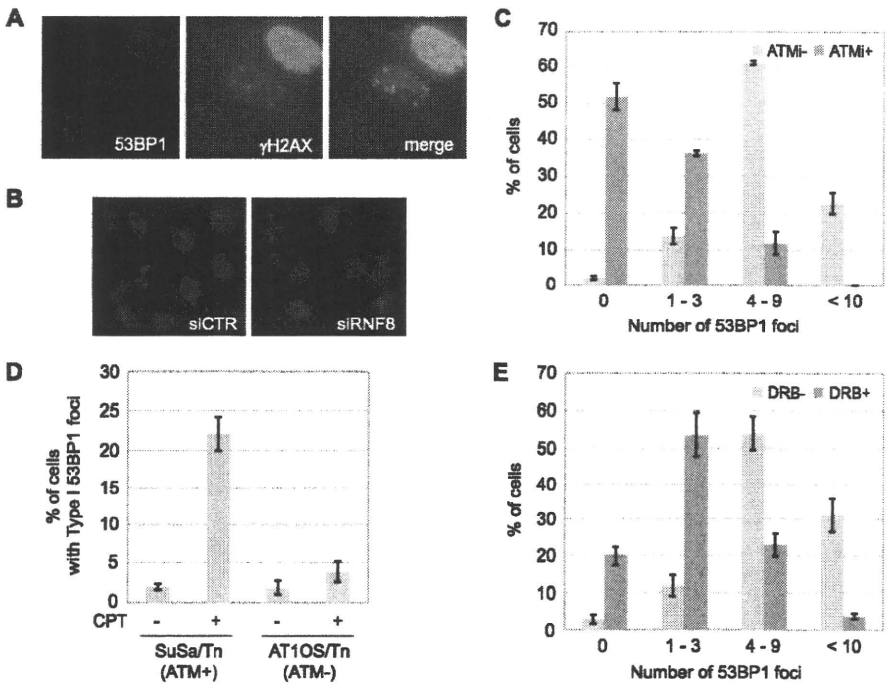

FIGURE 2. **Type I 53BP1 foci are ATM-dependent and occur in response to transcription-mediated DNA damage.** *A*, co-staining 53BP1 with γH2AX. HeLa cells were treated with CPT (2 μM, 1 h) and stained with α-53BP1 and γH2AX antibodies. *B*, formation of 53BP1 foci requiring RNF8. HeLa cells were transfected with nontargeting (*siCTR*) or RNF8-targeting siRNA (*siRNF8*) and stained with anti-53BP1 antibody following CPT (2 μM, 1 h) treatment. *C*, effect of ATM inhibition on Type I 53BP1 foci formation. HeLa cells were treated with solvent only, KU-55933 (10 μM, 1 h) before CPT (2 μM, 1 h) treatment, and stained with anti-53BP1 and anti-RPA2 antibodies. *D*, Type I 53BP1 foci in ATM-deficient cells. Control cells (*SuSa/Tn*) and ATM-deficient cells (*AT1OS/Tn*) were treated with CPT (2 μM, 1 h) and stained with anti-53BP1 and anti-RPA2 antibodies. *E*, effect of transcription inhibition on Type I 53BP1 foci formation. HeLa cells were treated with DRB (100 μM, 2 h) before CPT (2 μM, 1 h) treatment and stained with anti-53BP1 and anti-RPA2 antibodies. The number of 53BP1 foci observed in cells without RPA2 signal was counted. *Error bars* show S.E. calculated from three independent experiments.

many smaller foci (Fig. 1*A*). To characterize Type I and Type II foci further, we co-stained the cells with antibodies specific for the 32-kDa subunit of replication protein A (RPA2) following cellular preextraction with detergent. The presence of detergent-resistant RPA2 foci was used to distinguish S phase cells from G_1 phase cells (13). We found that cells possessing Type I 53BP1 foci were not co-stained for RPA2, whereas cells possessing Type II 53BP1 foci were (Fig. 1*B*). This finding suggested that Type I 53BP1 foci are formed predominantly in non-S phase cells. Consistent with this idea, cells displaying Type I 53BP1 foci did not incorporate BrdUrd, supporting the assertion that they are in either in G_1 or G_2/M phase (Fig. 1*B*). To substantiate this finding further, we used cell cycle synchronization to show that G_1 phase cells treated with CPT displayed Type I 53BP1 foci, whereas Type II 53BP1 foci were predominantly observed in S phase cells following CPT treatment (Fig. 1*C*). These results raised the possibility that Type I, DNA replication-independent, 53BP1 foci are caused by transcription-mediated DNA damage.

Formation of Type I 53BP1 Foci Requires RNF8, ATM, and Active Transcription—To characterize the CPT-induced Type I 53BP1 foci further, we examined co-localization of 53BP1 with a well established marker of DNA damage, phosphorylated-H2AX (γH2AX). We found that Type I foci were co-localized with γH2AX. On the other hand, γH2AX showed an intense, pan-nuclear signal in cells displaying Type II 53BP1 foci (Fig. 2*A*). The E3 ubiquitin ligase RNF8 is required for 53BP1 foci formation in response to DSBs induced by IR (14–16), and we found that RNF8 knockdown also sharply suppressed CPT-induced 53BP1 foci (Fig. 2*B* and supplemental Fig. S1). To test for the dependence of this response on ATM, HeLa cells were treated with the ATM inhibitor KU-55933 coincident with CPT treatment and co-stained with 53BP1 and RPA2. Focusing solely on RPA2-negative, non-S phase cells, we found that the number of Type I 53BP1 foci/cell was suppressed in KU-55933-treated cells as well as ATM-deficient cells (Fig. 2, *C* and *D*). These findings strongly suggested that Type I 53BP1 foci were formed in an ATM-dependent manner.

CPT interferes with RNA transcription, and transcription-associated DNA damage linked to ATM activation has recently been reported (7). Therefore, we tested the transcription dependence of CPT-induced 53BP1 foci by treating cells with DRB, a CDK inhibitor, that suppresses the phosphorylation of polymerase II C-terminal domain required for transcription elongation (17–19). Cells pretreated with DRB showed a drastic reduction in Type I 53BP1 foci (Fig. 2*E*). Taken together, these data demonstrate that, in non-S phase cells, CPT causes transcription-mediated DNA damage leading to the ATM and RNF8-dependent accumulation of 53BP1 foci.

Transcription-dependent ATM Activation in Response to CPT—The above experiments using DRB suggested that CPT-induced ATM activation is dependent on transcription. However, DNA replication-mediated DSEs are thought to account for the majority of CPT-induced DNA damage. To assess the relative contributions of transcription-associated *versus* replication-associated DNA damage to the activation of downstream pathways, HeLa cells were pretreated with inhibitors of DNA replication and transcription prior to the addition of CPT. Treatment with the replication inhibitor HU for 10 min effectively suppressed DNA synthesis (supplemental Fig. S2) and virtually abolished CPT-induced RPA2 phosphorylation (Fig. 3, *left*). Thymidine treatment prior to CPT addition also suppressed RPA2 phosphorylation (Fig. 3, *left*), indicating that RPA2 phosphorylation is highly dependent on DNA replication. In contrast, neither CPT-induced ATM autophosphorylation on Ser^{1981} nor ATM-dependent phosphorylation of Chk2 on Thr^{68} was suppressed by DNA replication inhibition

Downloaded from www.jbc.org at Tokyo Ikashika Daigaku, on February 27, 2011

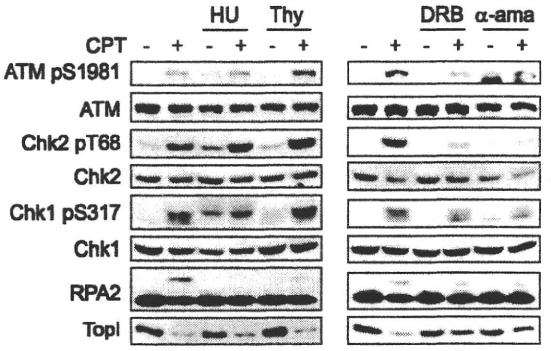

FIGURE 3. **Transcription-dependent ATM activation in response to CPT.** HeLa cells were pretreated with DNA replication inhibitors (HU and thymidine (Thy), 2 mM and 2.5 mM, respectively) or transcription inhibitors (DRB and α-amanitin, 100 μM and 5 μM, respectively) before CPT (2 μM, 1 h) treatment. DNA damage signaling was analyzed by Western blotting using appropriate antibodies.

(Fig. 3, *left*). These results imply that CPT-dependent activation of ATM does not absolutely require DNA replication.

In stark contrast to results using DNA replication inhibitors, the transcriptional inhibitors DRB and α-amanitin apparently suppressed CPT-induced ATM autophosphorylation at Ser^{1981} and Chk2 phosphorylation on Thr^{68} (Fig. 3, *right*). These results are consistent with previous reports demonstrating that CPT-induced ATM activation is dependent on transcription in non-cycling cells (7, 20). Our data further indicate that transcription-coupled events account for the bulk of ATM activation by CPT, even in actively dividing cells. Importantly, the transcription dependence of ATM activation established with CPT was not observed with other DNA-damaging agents, such as IR, the topoisomerase II inhibitor VP-16, and UV light (supplemental Fig. S3). These findings indicate that TopI poisons uniquely induce transcription-coupled DNA damage that signals to ATM.

ATM Is Required for CPT-induced Checkpoint Responses—To examine a possibility that ATM contributes to CPT-induced cell cycle checkpoint regulation, U2OS cells were treated with the ATM inhibitor KU-55933, exposed to CPT, and then monitored in cell cycle distribution by flow cytometry. Whereas U2OS cells treated with dimethyl sulfoxide or the DNA-PK inhibitor NU7026 exhibited prolonged G_1 arrest up to 12 h following CPT treatment, U2OS cells treated with KU-55933 began exiting G_1 phase by 6 h (Fig. 4*A*). This indicates that CPT induces an ATM-dependent G_1/S checkpoint. Consistent with a defect in the G_1/S phase checkpoint, ATM-inhibited U2OS cells rapidly accumulated in the S phase between 6 and 12 h after CPT treatment (Fig. 4*B*). By 24 h after CPT exposure, however, ATM-inhibited cells exited S phase and accumulated in the G_2 phase, which is indicative of a defect in S phase checkpoint maintenance (Fig. 4*B* and supplemental Fig. S4). In contrast, inhibition of DNA-PK did not result in S phase accumulation of U2OS cells at early time points (6–12 h), nor did the inhibitor cause premature S phase checkpoint release (Fig. 4*B*). Together, these results suggest that ATM, but not DNA-PK, is involved in CPT-induced G_1/S and S phase checkpoint activation.

Based on the ATM contribution to S phase checkpoint activation, we further analyzed the effect of ATM on the ATR-Chk1 pathway. Autophosphorylation of ATM Ser^{1981} and DNA-PKcs Ser^{2056} was used to monitor ATM and DNA-PK activation, respectively, whereas Chk1 Ser^{317} phosphorylation was used as a surrogate marker for ATR activation. Treatment with caffeine (2 mM) had no effect on ATM and DNA-PKcs autophosphorylation, but strongly suppressed Chk1 phosphorylation (supplemental Fig. S5), which is consistent with the previous finding that ATR is the primary Chk1-activating kinase in response to TopI poisons (4). ATM inhibition also strongly suppressed Chk1 phosphorylation, indicating that both ATM and ATR are required for full Chk1 activation in response to CPT (supplemental Fig. S5).

To analyze CPT-induced Chk1 phosphorylation further, we performed knockdown of TopBP1, a direct activator of ATR that is required for Chk1 phosphorylation in response to IR, UV, and HU (21). HeLa cells were transfected with siRNA against TopBP1, and the phosphorylation of Chk1, Chk2, and RPA2 was analyzed by Western blotting. CPT-induced Chk1 phosphorylation was suppressed in TopBP1 knockdown cells, whereas Chk2 phosphorylation was not (Fig. 4*C*), implying that CPT-induced Chk1 phosphorylation requires TopBP1 and suggesting that ATM is upstream of TopBP1 in the pathway leading to Chk1 phosphorylation. RPA2 phosphorylation was not suppressed by TopBP1 knockdown (Fig. 4*C*). Given that CPT-induced phosphorylation of RPA2 is reported to be ATR-dependent (22), this finding indicates that ATR can be activated independent of TopBP1 in CPT-treated cells. Finally, we used synchronized HeLa cells to show that CPT-induced TopBP1 and Chk1 phosphorylation are restricted to S phase cells and are dependent on ATM (Fig. 4*D*). From these findings, we propose the existence of an ATM-TopBP1-ATR-Chk1 signaling pathway that is activated by CPT in S phase cells. Because transcription inhibition only slightly affected CPT-induced Chk1 phosphorylation, replication-coupled DSEs, but not transcription-coupled DNA damage, probably trigger this pathway.

Hyperactivation of DNA-PK in ATM-inhibited Cells—The above findings are consistent with a model in which CPT caused the transcription-coupled activation of an ATM-dependent G_1/S checkpoint. Interestingly, we found that CPT-induced activation of DNA-PK was strongly potentiated when ATM was inhibited in HeLa cells (Fig. 5*A*). This result was also observed in ATM-deficient cells (Fig. 5*B*). The enhanced DNA-PKcs autophosphorylation observed in the presence of the ATM inhibitor KU-55933 was suppressed by HU treatment, indicating that DNA-PK hyperactivation by ATM inhibition requires ongoing DNA replication (Fig. 5*A*). This finding is consistent with our earlier report that CPT-induced DNA-PK activation is strongly dependent on DNA replication (23). DRB also partially inhibited CPT-induced DNA-PK autophosphorylation, which is consistent with the notion that transcription-coupled events lie upstream of DNA-PK activation (Fig. 5*A*).

A plausible explanation for the DNA replication and transcription-dependent hyperactivation of DNA-PK in ATM-inhibited cells is that ATM inhibition led to the defect in G_1/S and S phase checkpoints and the carryover of transcription-mediated strand breaks into the S phase, where such lesions were converted to frank DSEs activating DNA-PK. To test this possibility, we used neutral comet assays to assess CPT-induced

Downloaded from www.jbc.org at Tokyo Ikashika Daigaku, on February 27, 2011